Detection of the HIV-1 accessory proteins Nef and Vpu by flow cytometry represents a new tool to study their functional interplay within a single infected CD4+ T cell

Jérémie Prévost[1,2,*], Jonathan Richard[1,2,*], Romain Gasser[1,2], Halima Medjahed[1], Frank Kirchhoff[3], Beatrice H. Hahn[4], John C. Kappes[5], Christina Ochsenbauer[5], Ralf Duerr[6], Andrés Finzi[1,2,7,#]

[1]Centre de Recherche du CHUM, Montreal, Quebec, Canada
[2]Département de Microbiologie, Infectiologie et Immunologie, Université de Montréal, Montreal, Quebec, Canada
[3]Institute of Molecular Virology, Ulm University Medical Center, Ulm, Germany.
[4]Departments of Medicine and Microbiology, Perelman School of Medicine, University of Pennsylvania, Philadelphia, PA, USA
[5]Department of Medicine, University of Alabama at Birmingham, Birmingham, AL, USA
[6]Department of Microbiology, New York University School of Medicine, New York, NY, USA
[7]Department of Microbiology and Immunology, McGill University, Montreal, Quebec, Canada

*Contributed equally

[#]**Corresponding author:**
Andrés Finzi
Centre de recherche du CHUM (CRCHUM)
900 St-Denis street, Tour Viger, R09.420
Montréal, Québec, H2X 0A9, Canada
andres.finzi@umontreal.ca
Phone: 514-890-8000 ext: 35264
Fax: 514-412-7936

Running Title: Nef and Vpu expression dictates ADCC responses

Key Words: HIV-1, Env, Nef, Vpu, CD4, BST-2, ADCC

ABSTRACT

The HIV-1 Nef and Vpu accessory proteins are known to protect infected cells from antibody-dependent cellular cytotoxicity (ADCC) responses by limiting exposure of CD4-induced (CD4i) envelope (Env) epitopes at the cell surface. Although both proteins target the host receptor CD4 for degradation, the extent of their functional redundancy is unknown. Here, we developed an intracellular staining technique that permits the intracellular detection of both Nef and Vpu in primary CD4+ T cells by flow cytometry. Using this method, we show that the combined expression of Nef and Vpu predicts the susceptibility of HIV-1-infected primary CD4+ T cells to ADCC by HIV+ plasma. We also show that Vpu cannot compensate for the absence of Nef, thus providing an explanation for why some infectious molecular clones that carry a LucR reporter gene upstream of Nef render infected cells more susceptible to ADCC responses. Our method thus represents a new tool to dissect the biological activity of Nef and Vpu in the context of other host and viral proteins within single infected CD4+ T cells.

IMPORTANCE

HIV-1 Nef and Vpu exert several biological functions that are important for viral immune evasion, release and replication. Here, we developed a new method allowing simultaneous detection of these accessory proteins in their native form together with some of their cellular substrates. This allowed us to show that Vpu cannot compensate the lack of a functional Nef, which has implication for studies that use Nef-defective viruses to study ADCC responses.

57 **INTRODUCTION**

58 The human immunodeficiency virus type 1 (HIV-1) genome encodes four accessory proteins
59 (Vif, Vpr, Vpu and Nef), which are dispensable for viral replication *in vitro* but required
60 for efficient replication, restriction factors counteraction and immune evasion *in vivo* (1-
61 7). Among them, Nef and Vpu are well known for their role in subverting the host cell
62 protein trafficking machinery (8, 9).

63

64 HIV-1 Nef is a small cytoplasmic protein of 27 kDa produced from early viral transcripts (10),
65 which requires a myristoyl group on its N-terminus to traffic to intracellular and plasma
66 membranes (11). Nef harbors a highly conserved dileucine motif in its C-terminal flexible loop
67 that is responsible for the interaction with clathrin adaptors protein complexes (AP-1, AP-2 and
68 AP-3) (12). Among these, interaction with AP-2 is required to downregulate the CD4 receptor
69 from the surface of infected cells (13, 14) and target it for degradation in lysosomal
70 compartments (15, 16).

71

72 HIV-1 Vpu is a small type-I transmembrane protein of 16 kDa produced late in the viral
73 replication cycle (17, 18) and contains a short luminal N-terminal peptide followed by a single
74 helical transmembrane domain and a C-terminal cytoplasmic domain (19-21). The cytoplasmic
75 domain is comprised of two α-helices linked by a flexible loop known for its interaction with the
76 $SCF^{\beta TRCP}$ E3 ubiquitin ligase complex via a conserved phosphoserine motif ($DS^{P}GNES^{P}$) (22,
77 23). Vpu mainly localizes within intracellular compartments, notably the endoplasmic reticulum
78 (ER) and the *trans*-Golgi network (TGN) (24-26). Like Nef, Vpu also induces degradation of
79 newly synthesized CD4 by directing it through an ER-associated pathway (ERAD) for further

80 proteasomal degradation (22, 27-29). In addition, Vpu sequesters the restriction factor BST-2 in
81 the TGN using its transmembrane domain, thereby increasing the release of progeny virions (30-
82 33).
83
84 CD4 downregulation by Nef and Vpu was previously reported to be critical for efficient viral
85 replication in T cells by enhancing virion release and infectivity, and by preventing
86 superinfection (34-39). CD4 downregulation is critical for immune evasion since the anti-Env
87 antibody (Ab) response is dominated by non-neutralizing antibodies (nnAbs) that target Env in
88 its "open" CD4-bound conformation (40-42). The interaction between CD4 and Env at the
89 surface of HIV-1-infected cells has been shown to promote nnAbs binding to Env, leading to the
90 elimination of infected cells through Fc-mediated effector functions, including antibody-
91 dependant cellular cytotoxicity (ADCC) (41, 43). Nef and Vpu limit the presence of Env-CD4
92 complexes at the cell surface and thus protect infected cells against ADCC (41, 43, 44).
93
94 In previous studies, Nef and Vpu expression was mostly examined in transfected cell lines,
95 frequently using tagged proteins (30, 31, 45, 46) or by performing Western blots and
96 immunofluorescence microscopy in infected primary cells (47-52). However, both proteins are
97 small, intracellularly located and present in low amounts, rendering their detection difficult. To
98 facilitate their analysis in primary CD4+ T cells, we developed an intracellular staining technique
99 to detect Nef and Vpu expression by flow cytometry, which allows the simultaneous detection of
100 these proteins together with host and viral proteins within a single infected cell. Using this
101 method, we show that Nef and Vpu expression predicts the susceptibility of HIV-1-infected
102 primary CD4+ T cells to ADCC by HIV+ plasma. We also explain why decreased Nef

103 expression in widely-used reporter viruses increase the susceptibility of infected cells to ADCC
104 responses.
105
106 **RESULTS**
107 **Intracellular detection of Nef and Vpu in HIV-1-infected primary CD4+ T cells.**
108 To facilitate detection of intracellular Nef, we obtained a polyclonal Nef antiserum through the
109 NIH AIDS Reagent Program, which was generated by immunization of rabbits with a
110 recombinant clade B Nef consensus protein produced in *E. coli* (53). In previous studies, this
111 antibody detected native Nef proteins by Western blot and immunofluorescence microscopy in
112 both transfected and infected cells (47, 54-56). Given the scarcity of anti-Vpu antibodies, we
113 immunized rabbits with a peptide corresponding to the clade B Vpu C-terminal region (residues
114 69-81). A similar approach was previously used to generate a polyclonal antibody capable of
115 detecting Vpu by Western blot and immunofluorescence microscopy (24, 57).
116
117 We first evaluated the ability of both Nef and Vpu antisera to recognize their cognate antigen
118 using HEK 293T cells transfected with plasmids expressing the Nef or Vpu proteins from the
119 transmitted/founder (T/F) virus CH058 (58, 59). Forty-eight hours post-transfection, cells were
120 permeabilized and stained with the antisera, followed by detection with a fluorescently-labelled
121 anti-rabbit secondary antibody. As expected, the Nef antiserum recognized only Nef transfected
122 cells, while the Vpu antiserum recognized only Vpu transfected cells (Fig. 1A-C). To evaluate
123 whether our method detected Nef and Vpu when expressed in a biologically relevant culture
124 system, we infected primary CD4+ T cells with CH058 infectious molecular clones (IMC)
125 encoding Nef, and/or Vpu proteins. While wildtype (WT)-infected cells were efficiently

126 recognized by both Nef and Vpu antisera, abrogation of Nef (Fig 1D-E) or Vpu (Fig. 1F-G)
127 expression prevented the recognition of productively-infected cells as identified by Gag protein
128 intracellular staining (p24+). Of note, mock-infected or uninfected bystander cells (p24-) where
129 not detected by either antiserum, further confirming their specificity (Fig 1D-G).
130
131 We next examined the antiserum binding to Nef and Vpu proteins from different HIV-1 clades
132 and groups as well as from closely related simian immunodeficiency viruses (SIV). Primary
133 CD4+ T cells were infected with a panel of HIV-1 IMCs representing clades B, C, A1 and
134 CRF01_AE. As expected, both Nef and Vpu antisera recognized their respective antigen in cells
135 infected with clade B viruses since both were raised against clade B immunogens (Fig. 1H-I).
136 The anti-Nef polyclonal antibody was also able to recognize Nef proteins from group M clades
137 C, A1 and CRF01_AE as well as the Nef from a group O isolate. This recognition extended even
138 to the Nef protein of a related SIVcpzPts strain (isolate TAN2) but not to chimeric simian-human
139 immunodeficiency viruses (SHIV) which express a SIVmac Nef (Fig. 1H). The Vpu antiserum
140 was less cross-reactive and failed to detect Vpu from clade C viruses (Fig. 1I). These findings
141 confirmed the specificity and cross-reactivity of the intracellular detection of Nef and Vpu using
142 infected primary CD4+ T cells.
143
144 **Measuring CD4 and BST-2 downregulation in infected primary CD4+ T cells with or**
145 **without Nef and Vpu expression.**
146 The efficient detection of Nef and Vpu at the single cell level by flow cytometry allowed us to
147 combine this approach with the quantification of CD4 and BST-2 expression levels on the cell
148 surface. Productively-infected cells (p24+) expressing both Nef and Vpu had little detectable

149 CD4 and BST-2 compared to uninfected cells (Fig. 2A). In contrast, cells infected with Vpu or
150 Nef mutant viruses differed in the extent of CD4 and BST-2 downregulation (Fig. 2A).
151
152 Vpu targets CD4 and BST-2 by different mechanisms. First, Vpu interacts with multiple
153 transmembrane proteins, including BST-2, through its transmembrane domain (TMD), which
154 sequesters these proteins in perinuclear compartments (32, 33, 60-63). Second, Vpu
155 downregulates CD4 by interaction of its cytoplasmic domain with the cytoplasmic tail of CD4
156 (64-69). Consistent with these different interaction modes, Vpu-mediated CD4 and BST-2
157 degradation involves independent pathways (proteasomal and lysosomal degradation,
158 respectively), both of which depend on polyubiquitination by the $SCF^{\beta TRCP}$ E3 ubiquitin ligase
159 complex, recruited by Vpu using its highly conserved phosphoserine motif (22, 26, 70, 71). To
160 examine whether we could measure the expression and activity of Vpu mutants by flow
161 cytometry, we introduced mutations at critical residues of the Vpu TMD (A14L/A18L) or its
162 phosphoserine motif (S52A/S56A). CH058 IMCs coding for wildtype or mutated Vpu proteins
163 were used to infect primary CD4+ T cells. While the TMD mutations did not affect Vpu
164 expression, the phosphoserine mutations led to a significant accumulation of intracellular Vpu
165 proteins (Fig. 2B), most likely because Vpu is degraded together with its target protein as a
166 ubiquitinated complex (24, 72, 73). Despite a higher expression, the Vpu phosphoserine mutant
167 was unable to downregulate CD4 and marginally diminished in its capacity to antagonize BST-2
168 (Fig 2C-F). This is consistent with studies demonstrating that the recruitment of the $SCF^{\beta TRCP}$ E3
169 ubiquitin ligase complex and the degradation of BST-2 by Vpu is dissociable from its capacity to
170 antagonize the restriction factor (32, 71, 74-76). In contrast, the Vpu TMD mutations did not
171 affect Vpu's ability to target CD4 but completely abrogated its capacity to downregulate BST-2

172 (Fig 2C-F). Together, these results emphasize the need of measuring Nef and Vpu expression
173 when studying their biological functions.
174
175 **Nef and Vpu expression inversely correlates with ADCC responses.**
176 CD4 downregulation by Nef and Vpu, together with Vpu-mediated BST-2 antagonism were
177 found to be critical factors preventing the exposure of vulnerable CD4-induced Env epitopes,
178 thus protecting HIV-1-infected cells from ADCC (41, 43, 44, 77-80). To investigate the link
179 between Nef and Vpu expression and HIV-1-infected cells immune evasion, we infected
180 activated primary CD4+ T cells from five HIV-negative individuals with two clade B IMCs,
181 CH058 T/F and JR-FL, encoding functional or defective *nef* and *vpu* genes. Focusing on the
182 productively-infected cells (p24+), we performed a comprehensive characterization of the
183 patterns of viral protein expression including cell-surface Env (detected with the conformation-
184 independent Ab 2G12), intracellular Nef and Vpu in combination with cell-surface levels of CD4
185 and BST-2. We also measured the specific recognition and elimination of infected cells by
186 ADCC using the CD4-induced (CD4i) A32 monoclonal Ab (mAb). This antibody binds the
187 cluster A region of the gp120 which is occluded in the "closed" trimer and therefore can only
188 bind Env in the "open" CD4-bound conformation. We also tested 25 different plasma samples
189 from chronically HIV-1-infected individuals. As expected, Nef was only expressed by WT and
190 Vpu- constructs, while Vpu was only expressed by WT and Nef- constructs (Fig. 3A). Consistent
191 with previous reports (43, 77, 78), deletion of Nef strongly impaired CD4 downregulation by
192 both viruses but did not affect Env or BST-2 cell-surface levels. Vpu deletion mitigated CD4
193 downregulation to a lesser extent than Nef and abrogated BST-2 downmodulation, resulting in an
194 overall increase in the amount of cell-surface Env (Fig. 3B). We noticed lower levels of the JR-

195 FL Vpu protein compared to CH058 Vpu, which was linked to a less effective Vpu-mediated
196 CD4 downmodulation (Fig. 3B). The cumulative effect of Nef and Vpu on cell-surface levels of
197 Env, CD4 and BST-2 prevented the recognition of infected cells and protected them from ADCC
198 responses mediated by A32 and HIV+ plasma (Fig. 3C-D). In contrast, abrogation of Nef or Vpu
199 expression resulted in increased recognition and susceptibility of infected cells to ADCC
200 mediated by nnAbs (Fig. 3C-D). We performed correlation analyses to measure the level of
201 association between the different cellular, virological and immunological variables (Fig 3E-F).
202 We found that both Nef and Vpu established a large network of inverse correlations with cellular
203 and immunological factors. Interestingly, Env levels hardly contributed to the network and were
204 poorly associated with the immunological outcome, thus indicating that the overall amount of
205 Env present at the surface does not dictate ADCC responses mediated by CD4i Abs or HIV+
206 plasma, but rather the conformation Env occupies. Apart from antibody binding, ADCC
207 responses mediated by nnAbs correlated strongly with CD4 and Nef levels (Fig. 3E-F). Overall,
208 Nef and Vpu expression inversely correlates with the susceptibility of HIV-1-infected cells to
209 ADCC mediated by CD4i Abs and HIV+ plasma.
210

211 **Impaired Nef expression from IMC LucR.T2A constructs enhance the susceptibility of**
212 **infected cells to ADCC.**

213 Infectious molecular clones encoding for the *Renilla* luciferase (LucR) reporter gene upstream of
214 the *nef* sequence, and a T2A ribosome-skipping peptide to drive Nef expression are widely
215 employed to quantify anti-HIV-1 ADCC responses (81-92). Despite evidence that Nef-mediated
216 CD4 downregulation is impaired when using these IMCs (54, 79), a series of recent studies have
217 hypothesized that Vpu can compensate for the absence of Nef expression and completely

218 downregulate CD4 on its own (93-97). To evaluate this hypothesis, we used our intracellular
219 staining to measure Nef and Vpu expression levels and study their impact on ADCC responses
220 mediated by nnAbs against cells infected with IMC-LucR.T2A constructs. Primary CD4+ T cells
221 were infected with NL4.3-based IMCs that do (Env-IMC-LucR.T2A) or do not encode (Env-
222 IMC) a LucR.T2A cassette. These IMCs express the Env ectodomain from two clade B viruses,
223 CH058 T/F and YU-2. Consistent with the lack of Nef detection by Western blot (54, 79),
224 insertion of the LucR.T2A cassette also impaired the detection of Nef by flow cytometry, while
225 Vpu expression remained unchanged (Fig. 4A-B). However, we noted an accumulation of cell-
226 surface CD4 for Env-IMC-LucR.T2A compared to *nef*-intact constructs (~20-fold higher) (Fig.
227 4C), which resulted in a significantly increased recognition and susceptibility of infected cells to
228 ADCC responses mediated by A32 mAb and HIV+ plasma (Fig. 4D-E). Of note, both the
229 binding and the ADCC responses mediated by nnAbs were strongly associated with CD4 levels
230 and inversely correlated with Nef expression (Fig 4F-G). In contrast, these variables poorly
231 correlated with Vpu expression. Based on these data, it seems clear that Vpu expression alone is
232 not sufficient to prevent ADCC-mediated killing of infected cells and that HIV-1 requires both
233 Nef and Vpu for efficient humoral response evasion.
234

235 **Nef, Vpu and CD4 levels predict ADCC responses mediated by HIV+ plasma.**

236 We next used univariate multiple linear regression (MLR) analysis to evaluate the capacity of
237 different variables to predict ADCC responses mediated by HIV+ plasma. This model is based
238 on the hypothesis that a linear relationship exists between the dependant variable quantified
239 empirically and the independent variables that serve as predictive variables. In our model, the
240 dependant variable is the ADCC responses mediated by plasma from HIV+ donors (ADCC

241 HIV+ plasma) and the independent variables are the cellular, virological and immunological
242 factors measured on infected cells. To run the MLR model, we combined data obtained with the
243 different viral constructs (Fig. 3 & 4) and plotted the mean ADCC obtained with 25 HIV+
244 plasma against a single virus on the X axis and the associated predicted ADCC value based on
245 one or more independent variables on the Y axis. When looking at cellular factors, we noticed
246 that only CD4 accurately predicts ADCC responses mediated by HIV+ plasma, independent of
247 the viral strain (Fig. 5A). Even though BST-2 displayed a strong correlation with ADCC
248 responses (Fig 3E), it was not predictive. When focusing on virological variables, we observed
249 that Nef is the only significant ADCC predictive variable, albeit not as good as CD4 (Fig. 5A-B).
250 However, combinations of Nef with Vpu or Env increased its predictive scores, reaching similar
251 levels as CD4 when combined with Vpu (Fig. 5B). Of note, the strength of the prediction was not
252 further improved when combining all three virological variables altogether. As for
253 immunological variables, their capacity to predict ADCC by HIV+ plasma was found to be
254 equivalent or even higher than for cellular and virological factors (Fig. 5C). Indeed, the binding
255 of HIV+ plasma predicted ADCC values with a similar score as CD4 or Nef and Vpu combined,
256 while the binding of A32 predicted ADCC by HIV+ plasma even better (Fig. 5A-C). This could
257 be explained by the fact that A32-like Abs present in plasma from infected individuals are from
258 the main class of Abs (anti-cluster A Abs) mediating ADCC responses against infected cells (41,
259 80, 81, 91, 98). In line with this interpretation, ADCC mediated by A32 was found to have a
260 near-perfect predictive ability, suggesting that factors, other than antibody binding, are
261 presumably needed to fully explain the ADCC phenotypes observed (Fig. 5C).
262
263

264 **DISCUSSION**

265 Unlike simple retroviruses, HIV-1 and related SIVs encode multiple accessory proteins that
266 promote viral replication and immune evasion (99). Among them, Nef and Vpu modulate the
267 expression, trafficking, localization and function of several host cell surface proteins, including
268 the viral receptor CD4, restriction factors and homing receptors (28, 30, 31, 62, 69, 100-104).
269 They also modulate a wide range of immunoreceptors to evade immune responses mediated by
270 CD8+ T, NK and NKT cells (105-113) . Most of these host cell proteins are naturally expressed
271 on primary CD4+ T cells, the preferential target of HIV-1. The detection of Nef and Vpu has
272 previously been done in transfected cells (30, 31, 46, 48, 49, 114), which results in the
273 overexpression of the viral proteins when compared to infected primary CD4+ T cells.
274 Moreover, tagged viral proteins are frequently used to facilitate their detection (30, 31, 46, 48,
275 49, 114). Protein overexpression and/or tag insertion, have the potential to impact the trafficking
276 and functions of these accessory proteins. To study Nef and Vpu's biological activities in a
277 physiologically relevant system, we developed an intracellular staining method to detect native
278 Nef and Vpu proteins in HIV-1-infected primary CD4+ T cells by flow cytometry. Using Nef
279 and Vpu antisera, we detected both viral proteins with high specificity in cells productively
280 infected (p24+) with multiple IMCs. The Nef antiserum was cross-reactive, detecting Nef from
281 group M (clade B, C, A1 and CRF01_AE), from a group O isolate and from a closely related
282 SIVcpz strain. In contrast, the Vpu antiserum recognized only clade B Vpu proteins, consistent
283 with the fact that we used a peptide from the C-terminal region of clade B Vpu. This region is
284 highly variable among group M viruses (Fig. S1). More conserved regions of Vpu map to the
285 transmembrane domain of the protein and the βTRCP binding site (115, 116). However, these
286 regions are either buried into the plasma membrane or occluded by cellular partners, and thus are

287 not readily accessible for antibody recognition. While the generation of a broad Vpu antiserum is
288 challenging, it may be possible to generate clade-specific Vpu antisera by immunization using
289 peptides corresponding to the C-terminal region specific for a given clade.
290
291 Nef and Vpu intracellular detection by flow cytometry represents an excellent tool to study their
292 biological activities in HIV-1-infected primary CD4+ T cells. This method allows for the
293 detection of cell-surface substrates or antibody recognition of surface Env and the concomitant
294 detection of Nef and Vpu expression within a single infected cell (Fig. 2A). Infected CD4+ T
295 cells represent the most relevant system to study the complex interplay between these two
296 accessory proteins and the wide range of host cell factors naturally expressed by T cells. Recent
297 findings revealed that modulation of BST-2 levels by type I IFN impacts the capacity of Vpu to
298 downregulate NTB-A, PVR, CD62L and Tim-3, thus reducing its polyfunctionality (63, 69). Nef
299 and Vpu also display overlapping functions, as they share the capacity to downregulate several
300 cell-surface proteins, including CD4, PVR, CD62L and CD28 (8, 56, 62, 110, 117). The
301 expression levels of one viral protein could therefore modulate the biological activities of the
302 other, making it essential to study their functions in a context where both viral proteins are
303 expressed simultaneously at physiological levels. Thus, our intracellular staining measuring
304 Nef/Vpu expression and functionality in HIV-1-infected cells represents a new approach to better
305 characterize their functional interplay.
306
307 Increasing evidence points towards Env conformation on the surface of infected cells as a critical
308 parameter of ADCC susceptibility to HIV+ plasma (41, 118-120). Non-neutralizing antibodies in
309 the plasma from HIV-1-infected individuals target epitopes that are only exposed when Env

310 interacts with cell-surface CD4, thus adopting the "open" CD4-bound conformation (41, 43). Nef
311 and Vpu contribute to protect HIV-1-infected cells from ADCC by limiting Env-CD4 interaction
312 via CD4 downregulation and BST-2 antagonism (41, 43, 44, 77, 78). Here we confirm and
313 extend previous observations by showing that Nef and Vpu expression predicts the susceptibility
314 of HIV-1-infected primary CD4+ T cells to ADCC responses. In agreement with recent studies
315 (44, 79), we found that CD4 accurately predicted the susceptibility of infected cells to ADCC
316 (Fig. 5). Given its enhanced capacity to downregulate CD4 compared to Env or Vpu (34, 41, 43,
317 117), Nef represents the main viral factor influencing ADCC responses mediated by CD4-
318 induced ligands (Fig. 5B). On the contrary, BST-2 and Env expression, alone or in combination,
319 were unable to accurately predict the susceptibility of infected cells to ADCC. These results are
320 consistent with previous reports suggesting that Env conformation rather than overall cell-
321 surface Env levels, drives ADCC responses mediated by HIV+ plasma (41, 43, 119, 120). This is
322 also in agreement with recent work showing that BST-2 upregulation by type I IFN enhances
323 cell-surface Env levels without increasing the susceptibility of infected cells to ADCC mediated
324 by HIV+ plasma, unless CD4-mimetics are used to "open-up" Env and stabilize the CD4-bound
325 conformation (121).
326
327 A series of recent studies using LucR.T2A IMCs have hypothesized that Vpu can compensate for
328 the absence of Nef expression by fully downregulating cell-surface CD4 (93-97). Our results
329 show that this is not the case. Consistent with its role in targeting CD4 already present at the
330 plasma membrane, the impact of Nef on CD4 downmodulation is more prominent (Fig. 2 & 3)
331 (34, 41, 43, 117). In its absence, Vpu was unable to fully downregulate CD4, thus sensitizing
332 infected cells to ADCC responses. These results highlight the importance to select IMCs for

333 ADCC measurement with proper Nef and Vpu expression. Several alternatives to the use of
334 LucR.T2A IMCs are available to measure ADCC against productively-infected cells (122),
335 including the Infected Cell Elimination (ICE) assay, which measures the loss of productively-
336 infected cells (p24+) by flow cytometry and allows the utilization of unmodified IMCs.
337 Utilization of an NK cells resistant T cell line expressing a Tat-driven luciferase reporter gene
338 (CEM.NKr-CCR5-sLTR-Luc) as target cells also represents an option (123). Finally, luciferase
339 reporter IMCs (referred to as LucR.6ATRi IMCs) expressing similar levels of Nef than those
340 obtained with unmodified IMC are also available. These IMCs utilize a modified
341 encephalomyocarditis virus (EMCV) internal ribosome entry site (IRES) element in lieu of T2A
342 (54, 79). Thus, LucR.6ATRi reporter viruses represent a biologically relevant alternative to
343 LucR.T2A IMCs when measuring ADCC mediated by nnAbs and plasma collected from
344 infected or vaccinated individuals.
345

346 **ACKNOWLEDGMENTS**

347 The authors thank the CRCHUM BSL3 and Flow Cytometry Platforms for technical assistance,
348 Mario Legault from the FRQS AIDS and Infectious Diseases network for cohort coordination
349 and clinical samples. We thank the following collaborators for kindly providing some infectious
350 molecular clones: Dennis Burton (The Scripps Research Institute) for JR-FL, Malcom A. Martin
351 (NIAID) for $SHIV_{AD8-EO}$, George M. Shaw (UPenn) for SHIV.AE.40100 and Sodsai
352 Tovanabutra (US MHRP) for the HIV-1_{WR27}, HIV-1_{703357}, HIV-1_{40061}, HIV-1_{CM235} and HIV-
353 1_{851891} IMCs. We thank MédiMabs for their scientific and technical support during the
354 development of the Vpu antiserum. This work was supported by a CIHR foundation grant
355 #352417 and a CIHR Team grant #422148 to A.F. Support for this work was also provided by

grants from the National Institutes of Health to A.F., C.O. and J.C.K. (R01 AI148379), to A.F. (R01 AI129769 and R01 AI150322) and to BHH (R01 AI162646 and UM1 AI164570), and by NIAID-funded ERASE HIV consortium (UM1 AI164562) to A.F. A.F. is the recipient of a Canada Research Chair on Retroviral Entry #RCHS0235 950-232424. F.K. is supported by the Deutsche Forschungsgemeinschaft (CRC 1279 and SPP 1923). J.P. is the recipient of a CIHR doctoral fellowship. The funders had no role in study design, data collection and analysis, decision to publish, or preparation of the manuscript.

AUTHOR CONTRIBUTIONS

J.P. J.R. and A.F. conceived the study. J.P., J.R., and A.F. designed experimental approaches. J.P., J.R., R.G. R.D. and A.F. performed, analyzed, and interpreted the experiments. H.M., F.K., B.H.H., J.C.K. and C.O. supplied novel/unique reagents. J.P., J.R., BHH, and A.F. wrote the paper. All authors have read, edited, and approved the final manuscript.

CONFLICT OF INTEREST

The authors declare no competing interests.

373 **METHODS**

374

375 **Ethics Statement**

376 Written informed consent was obtained from all study participants [the Montreal Primary HIV
377 Infection Cohort (124, 125) and the Canadian Cohort of HIV Infected Slow Progressors (126-
378 128), and research adhered to the ethical guidelines of CRCHUM and was reviewed and
379 approved by the CRCHUM institutional review board (ethics committee, approval number CE
380 16.164 - CA). Research adhered to the standards indicated by the Declaration of Helsinki. All
381 participants were adult and provided informed written consent prior to enrolment in accordance
382 with Institutional Review Board approval.

383

384 **Cell lines and isolation of primary cells**

385 HEK293T human embryonic kidney cells (obtained from ATCC) were grown as previously
386 described (129). Primary human PBMCs and CD4+ T cells were isolated, activated and cultured
387 as previously described (43). Briefly, PBMCs were obtained by leukapheresis from HIV-
388 negative individuals (4 males and 1 female) and CD4+ T lymphocytes were purified from resting
389 PBMCs by negative selection using immunomagnetic beads per the manufacturer's instructions
390 (StemCell Technologies, Vancouver, BC) and were activated with phytohemagglutinin-L (10
391 μg/mL) for 48 hours and then maintained in RPMI 1640 complete medium supplemented with
392 rIL-2 (100 U/mL).

393

394 **Plasmids and proviral constructs**

395 The vesicular stomatitis virus G (VSV-G)-encoding plasmid was previously described (130).

396 Transmitted/Founder (T/F) and chronic infectious molecular clones (IMCs) of patients CH040,
397 CH058, CH077, CH131, CH141, CH167, CH185, CH198, CH236, CH269, CH293, CH440,
398 CH470, CH505, CH534, CH850, CM235, MCST, REJO, RHGA, RHPA, STCO, SUMA, TRJO,
399 WARO, WITO, WR27, 40061, 703357 and 851891 were inferred, constructed, and biologically
400 characterized as previously described (119, 131-140). The IMCs encoding for HIV-1 reference
401 strains AD8, JR-FL, JR-CSF, NL4-3, YU-2 were described elsewhere (141-146). HIV-1 group O
402 (RBF206), SIVcpz (TAN2) and chimeric SIVmac/HIV-1 IMC constructs ($SHIV_{AD8-EO}$ and
403 SHIV.AE.40100) were generated as previously published (147-150). CH058 IMCs defective for
404 Vpu and/or Nef expression were previously described (58). To generate a *nef*-defective JR-FL
405 IMC, a frameshift mutation was introduced at the unique XhoI restriction site within the *nef*
406 gene, resulting in a premature stop codon at position 47. To generate *vpu*-defective JR-FL IMCs,
407 two stop-codons were introduced directly after the start-codon of *vpu* using the QuikChange II
408 XL site-directed mutagenesis protocol (Stratagene). The presence of the desired mutations was
409 determined by automated DNA sequencing. Proviral constructs, collectively referred as Env-
410 IMCs, comprising an HIV-1 NL4.3-based isogenic backbone engineered for the insertion of
411 heterologous *env* strain sequences and expression in *cis* of full-length Env (pNL.CH058.ecto and
412 pNL.YU-2.ecto), were previously described (47). In the same study, isogenic proviral constructs
413 encoding *Renilla* luciferase (LucR) followed in frame by a ribosome-skipping T2A peptide
414 intended to drive Nef expression were also reported (collectively referred to as Env-IMC-
415 LucR.T2A) (47). Construction of plasmids encoding for CH058 Vpu and CH058 Nef in the
416 pCGCG-IRES-eGFP expression vector was previously described (58, 59).
417
418 **Viral production and infections**

419 To achieve a similar level of infection in primary $CD4^+$ T cells among the different IMCs tested,
420 VSV-G-pseudotyped HIV-1 viruses were produced and titrated as previously described (119).
421 Viruses were then used to infect activated primary CD4+ T cells from healthy HIV-1 negative
422 donors by spin infection at 800 × *g* for 1 h in 96-well plates at 25 °C.
423
424 **Antibodies and plasma**
425 The following Abs were used to assess cell-surface Env staining: A32, 2G12 (NIH AIDS
426 Reagent Program) and PGT135 (IAVI). Mouse anti-human CD4 (clone OKT4; eBioscience) and
427 mouse anti-human BST-2 (clone RS38E, PE-Cy7-conjugated; Biolegend) were also used as
428 primary antibodies for cell-surface staining. Goat anti-mouse and anti-human antibodies pre-
429 coupled to Alexa Fluor 647 (Invitrogen) were used as secondary antibodies in flow cytometry
430 experiments. Plasma from HIV-infected individuals were collected, heat-inactivated and
431 conserved at −80 °C until use. Rabbit antisera raised against a Nef consensus protein (NIH AIDS
432 Reagent Program) or against a Vpu C-terminal peptide (69) were used as primary antibodies in
433 intracellular staining. BrillantViolet 421 (BV421)-conjugated donkey anti-rabbit antibodies
434 (Biolegend) were used as secondary antibodies to detect Nef and Vpu antisera binding by flow
435 cytometry. To avoid any potential cross-reactivity with the anti-rabbit secondary antibodies used
436 for intracellular staining, mouse monoclonal antibodies were used to detect CD4 and BST-2
437 proteins.
438
439 **Flow cytometry analysis of cell-surface and intracellular staining**
440 Cell-surface staining of infected cells was performed as previously described (41). Binding of
441 cell-surface HIV-1 Env by anti-Env mAbs (5 µg/mL) or HIV+ plasma (1:1000 dilution) was

442 performed at 48h post-infection. Infected cells were then permeabilized using the
443 Cytofix/Cytoperm Fixation/ Permeabilization Kit (BD Biosciences, Mississauga, ON, Canada)
444 and stained intracellularly using PE-conjugated mouse anti-p24 mAb (clone KC57; Beckman
445 Coulter; 1:100 dilution) in combination with Nef or Vpu rabbit antisera (1:1000 dilution). The
446 percentage of infected cells ($p24^+$) was determined by gating on the living cell population
447 according to a viability dye staining (Aqua Vivid, Thermo Fisher Scientific). Alternatively,
448 intracellular staining was assessed on 293T expressing Nef or Vpu proteins. Briefly, $2x10^6$ 293T
449 cells were transfected with 7ug of Nef or Vpu expressor with the calcium-phosphate method. At
450 48 h post transfection, 293T cells were stained intracellularly with rabbit antisera raised against
451 Nef or Vpu (1:1000). Samples were acquired on an LSRII cytometer (BD Biosciences), and data
452 analysis was performed using FlowJo v10.5.3 (Tree Star).
453
454 **FACS-based ADCC assay**
455 Measurement of ADCC using the FACS-based assay was performed at 48h post-infection as
456 previously described (43, 118). Briefly, HIV-1-infected primary CD4+ T cells were stained with
457 AquaVivid viability dye and cell proliferation dye (eFluor670; eBioscience) and used as target
458 cells. Autologous PBMC effectors cells, stained with another cellular marker (cell proliferation
459 dye eFluor450; eBioscience), were added at an effector: target ratio of 10:1 in 96-well V-bottom
460 plates (Corning, Corning, NY). A 1:1000 final dilution of plasma or 5µg/mL of A32 mAb was
461 added to appropriate wells and cells were incubated for 5 min at room temperature. The plates
462 were subsequently centrifuged for 1 min at 300 *x* g, and incubated at 37°C, 5% CO_2 for 5h before
463 being fixed in a 2% PBS-formaldehyde solution. Samples were acquired on an LSRII cytometer
464 (BD Biosciences) and data analysis was performed using FlowJo v10.5.3 (Tree Star). The

465 percentage of ADCC was calculated with the following formula: (% of p24+ cells in Targets plus
466 Effectors) − (% of p24+ cells in Targets plus Effectors plus plasma) / (% of p24+ cells in
467 Targets) by gating on infected lived target cells.
468

469 **Software Scripts and Visualization**

470 Correlograms were generated using the corrplot package in program R v.4.1.012 and RStudio
471 v.1.4.1106 (151, 152) . Correlation networks were created using the ggraph and igraph packages
472 in R in undirected mode, clustered based on the igraph layout "star". Edges are weighted
473 according to P-values (inversely). Edges are only shown if $P < 0.05$, and nodes without edges
474 were removed. Nodes are sized according to the r-values of connecting edges. Multiple linear
475 regression analyses were performed using the GraphPad Prism software (version 9.1.0). The
476 coefficient of determination (R^2) was used as a metric to measure the proportion of the variation
477 observed with the dependant variable that can be explained by the variation in the independent
478 variables. Since R^2 values usually increases when more predictive variables are added to the
479 model, we also measured the adjusted R^2 (adj. R^2) to account for this caveat.
480

481 **Sequence analysis**

482 The LOGO plots (153) were created using the Analyze Align tool at the Los Alamos National
483 Laboratory - HIV database and are based on the WebLogo program
484 (https://www.hiv.lanl.gov/content/sequence/ANALYZEALIGN/analyze_align.html) and the
485 HIV-1 database global curated and filtered 2019 alignment, including 5,292 individual Vpu
486 protein sequences. The relative height of each letter within individual stack represents the
487 frequency of the indicated amino acid at that position. The numbering of all the Vpu amino acid

488 sequences is based on the HXBc2 reference strain of HIV-1, where 1 is the initial methionine.

489

490 **Statistical analysis**

491 Statistics were analyzed using GraphPad Prism version 9.1.0 (GraphPad, San Diego, CA, USA).
492 Every data set was tested for statistical normality and this information was used to apply the
493 appropriate (parametric or nonparametric) statistical test. P values <0.05 were considered
494 significant; significance values are indicated as * P<0.05, ** P<0.01, *** P<0.001, ****
495 P<0.0001.

496

497 **FIGURE LEGENDS**

498

499 **Figure 1. Intracellular detection of Nef and Vpu in infected primary CD4+ T cells.**

500 (**A-C**) 293T cells transfected with an empty vector or a plasmid expressing either CH058 Nef or
501 CH058 Vpu. 48 hours post-transfection, cells were permeabilized and stained with rabbit
502 polyclonal antisera raised against Nef and Vpu to detect their respective intracellular expression.
503 Antiserum binding was detected using donkey anti-rabbit BV421 secondary Abs. (**A**) Histograms
504 depicting representative staining and (**B-C**) Median fluorescence intensities (MFI) obtained for
505 multiple independent stainings using (**B**) anti-Nef or (**C**) anti-Vpu. (**D-G**) Primary CD4+T cells
506 mock-infected or infected with CH058 T/F WT, Nef- or Vpu-, were stained to detect the
507 intracellular expression of Nef or Vpu. (**D,F**) Dot plots (left) and histograms (right) depicting
508 representative (**D**) Nef and (**F**) Vpu staining. (**E,G**) The graphs show the MFI obtained from
509 different cell populations using cells from five different donors using (**E**) anti-Nef or (**G**) anti-
510 Vpu. Error bars indicate means ± standard errors of the means (SEM). Statistical significance
511 was tested using an unpaired t test or a Mann-Whitney U test based on statistical normality (*,
512 $P < 0.05$; **, $P < 0.01$; ***, $P < 0.001$; ns, nonsignificant). (**H-I**) Primary CD4+ T cells were
513 infected with a panel of viruses from different clades (A1, B, C, CRF01_AE), group (M, O) and
514 host (HIV-1, SIVcpz, SHIV). The radar plots indicate the level of specific recognition of infected
515 cells (MFI normalized to uninfected cells) using the (**H**) anti-Nef or (**I**) anti-Vpu antisera. The
516 limit of detection was determined using (**H**) cells infected with CH058 Nef- for Nef staining and
517 using (**I**) cells infected with CH058 Vpu- for Vpu staining.

518

519 **Figure 2. Concomitant detection of intracellular Nef and Vpu and cell-surface CD4 and**
520 **BST-2.**
521 Primary CD4+T cells infected with CH058 T/F WT, Nef-, Vpu-, Vpu A14L/A18L or Vpu
522 S52A/S56A viruses were stained for cell-surface CD4 and BST-2 prior to detection of
523 intracellular Nef or Vpu expression. (**A,C,E**) Contour plots depicting representative cell-surface
524 CD4 or BST-2 detection in combination with Nef or Vpu intracellular detection. Mock-infected
525 cells were used as a control and are shown in grey. (**B,D,F**) The graphs show MFIs obtained
526 from five independent experiments. Error bars indicate means ± standard errors of the means
527 (SEM). Statistical significance was tested using an unpaired t test or a Mann-Whitney U test
528 based on statistical normality (*, $P < 0.05$; **, $P < 0.01$; ***, $P < 0.001$; ns, nonsignificant).
529
530 **Figure 3. Nef and Vpu intracellular detection inversely correlates with the recognition of**
531 **infected cells and their susceptibility to ADCC responses mediated by HIV+ plasma.**
532 Primary CD4+T cells were mock-infected (grey), infected with CH058 T/F (red) or JR-FL (Blue)
533 viruses (WT, Nef-, Vpu-, Nef- Vpu-) and stained for (**A**) intracellular Nef or Vpu expression in
534 combination with (**B**) cell-surface staining of Env (using the anti-Env 2G12 mAb), CD4 and
535 BST-2. The ability of the anti-Env A32 mAb and 25 different HIV+ plasma to (**C**) recognize
536 infected cells and (**D**) eliminate infected cells by ADCC was also measured. (**A-D**) The graphs
537 show the MFI obtained on the infected (p24+) cell population using cells from five different
538 donors. Error bars indicate means ± standard errors of the means (SEM). Statistical significance
539 was tested using an unpaired t test or a Mann-Whitney U test based on statistical normality (*,
540 $P < 0.05$; **, $P < 0.01$; ***, $P < 0.001$; ns, nonsignificant). (**E**) Correlograms summarize pairwise
541 correlations among all immunological, virological and cellular variables obtained from infected

542 primary CD4+ T cells (shown in A-D). Squares are color-coded according to the magnitude of
543 the correlation coefficient (r) and the square dimensions are inversely proportional with the P-
544 values. Red squares represent a positive correlation between two variables and blue squares
545 represent negative correlations. Asterisks indicate all statistically significant correlations (*P <
546 0.05, **P < 0.01, ***P < 0.005). Correlation analysis was done using nonparametric Spearman
547 rank tests. (**F**) Correlation networks were generated using data shown in (**E**). Each node (circle)
548 represents a cellular (red), an immunological (green) or a virological (blue) feature measured on
549 infected cells. Nodes are connected with edges (lines) if they are significantly correlated (P <
550 0.05); nodes without edges were removed. Edges are weighted according to P-values (inversely).
551 Red edges represent a positive correlation between two variables and blue edges represent
552 negative correlations. Nodes are sized according to the r-values of connecting edges.
553

554 **Figure 4. Lack of Nef expression in primary CD4+ T cells infected with LucR.T2A IMCs**
555 **results in enhanced ADCC.**

556 Primary CD4+T cells mock-infected (grey) or infected with chimeric IMCs expressing CH058
557 Env (red) or YU-2 Env (green) and expressing or not the LucR reporter gene. (**A**) Dot plots
558 depicting representative stainings of intracellular Nef or Vpu expression. (**B-C**) Detection by
559 flow cytometry of (**B**) intracellular Nef or Vpu expression in combination with (**C**) cell-surface
560 staining of Env (using anti-Env mAbs 2G12 (CH058) or PGT135 (YU-2)), CD4 and BST-2. The
561 ability of the A32 mAb and 25 HIV+ plasma to (**D**) recognize infected cells and (**E**) eliminate
562 infected cells by ADCC was also measured. (**B-E**) The graphs show the MFI obtained on the
563 infected (p24+) cell population using cells from five different donors. Error bars indicate means
564 ± standard errors of the means (SEM). Statistical significance was tested using an unpaired t test

565 or a Mann-Whitney U test based on statistical normality (*, $P < 0.05$; **, $P < 0.01$; ***,
566 $P < 0.001$; ns, nonsignificant). (**F**) Correlograms summarize pairwise correlations among all
567 immunological, virological and cellular variables obtained from infected primary CD4+ T cells
568 (shown in **B-E**). Squares are color-coded according to the magnitude of the correlation
569 coefficient (r) and the square dimensions are inversely proportional with the P-values. Red
570 squares represent a positive correlation between two variables and blue squares represent
571 negative correlations. Asterisks indicate all statistically significant correlations (*$P < 0.05$, **$P <$
572 0.01, ***$P < 0.005$). Correlation analysis was done using nonparametric Spearman rank tests.
573 (**G**) Correlation networks were generated using data shown in (**F**). Each node (circle) represents
574 a cellular (red), an immunological (green) or a virological (blue) feature measured on infected
575 cells. Nodes are connected with edges (lines) if they are significantly correlated ($P < 0.05$); nodes
576 without edges were removed. Edges are weighted according to P-values (inversely). Red edges
577 represent a positive correlation between two variables and blue edges represent negative
578 correlations. Nodes are sized according to the r-values of connecting edges.
579

580 **Figure 5. Prediction of ADCC responses mediated by HIV+ plasma using multiple linear**
581 **regression models.**

582 (**A-C**) Multiple linear regression analysis to identify variables that can predict the ADCC
583 responses mediated by HIV+ plasma against primary CD4+ T cells infected by different viral
584 constructs (WT, Nef-, Vpu-, Nef-Vpu-, Env-IMC, Env-IMC-LucR.T2A) from different HIV-1
585 strains (CH058, JR-FL, YU-2). Each dot represents a single virus where the average of ADCC
586 obtained with 25 different HIV+ plasma (dependent variable) is plotted on the X axis and the
587 predicted ADCC value based on one or more independent parameters is plotted on the Y axis.

588 Predictors include (**A**) cellular variables, (**B**) virological variables and (**C**) immunological
589 variables. Multiple linear regression analyses were performed using the GraphPad Prism
590 software (version 9.1.0). P values below 0.05 are considered significant and are highlighted in
591 bold. The coefficient of multiple correlation (R^2) indicates the goodness of fit of the multiple
592 regression linear model. The adjusted R^2 (Adj. R^2) is used to compare the fits of models across
593 experiments with different numbers of data points and independent variables.
594
595 **Figure S1. Sequence alignment of Vpu C-terminal region from HIV-1 major clades.**
596 (**A-H**) Logo depictions of the frequency of each amino acid from the Vpu C-terminal region
597 (residues 70-82) in isolates from (**A**) clade B, (**B**) clade C, (**C**) clade A1, (**D**) clade D, (**E**) clade
598 F1, (**F**) clade G, (**G**) CRF01_AE and (**H**) CRF02_AG. The height of the letter indicates its
599 frequency within the clade. The residues corresponding to the immunogen used to generate the
600 rabbit Vpu antiserum are highlighted in blue. The 2019 Los Alamos database-curated filtered
601 web Vpu alignment was used as the basis for this figure, which contains 5,292 amino acid HIV-1
602 group M sequences (including 1,819 sequences of subtype B, 1,075 of subtype C, 247 of subtype
603 A1, 87 of subtype D, 47 of subtype F1, 80 of subtype G, 397 of CRF01_AE and 139 of
604 CRF02_AG). Residue numbering is based on the HXBc2 reference strain of HIV-1.
605
606

607 **REFERENCES**

608 1. Desrosiers RC, Lifson JD, Gibbs JS, Czajak SC, Howe AY, Arthur LO, Johnson RP.
609 1998. Identification of highly attenuated mutants of simian immunodeficiency virus. J
610 Virol 72:1431-7.
611 2. Dave VP, Hajjar F, Dieng MM, Haddad E, Cohen EA. 2013. Efficient BST2 antagonism
612 by Vpu is critical for early HIV-1 dissemination in humanized mice. Retrovirology 10:128.
613 3. Sato K, Misawa N, Fukuhara M, Iwami S, An DS, Ito M, Koyanagi Y. 2012. Vpu
614 augments the initial burst phase of HIV-1 propagation and downregulates BST2 and
615 CD4 in humanized mice. J Virol 86:5000-13.
616 4. Sato K, Misawa N, Iwami S, Satou Y, Matsuoka M, Ishizaka Y, Ito M, Aihara K, An DS,
617 Koyanagi Y. 2013. HIV-1 Vpr accelerates viral replication during acute infection by
618 exploitation of proliferating CD4+ T cells in vivo. PLoS Pathog 9:e1003812.
619 5. Crotti A, Neri F, Corti D, Ghezzi S, Heltai S, Baur A, Poli G, Santagostino E, Vicenzi E.
620 2006. Nef alleles from human immunodeficiency virus type 1-infected long-term-
621 nonprogressor hemophiliacs with or without late disease progression are defective in
622 enhancing virus replication and CD4 down-regulation. J Virol 80:10663-74.
623 6. Rucker E, Grivel JC, Munch J, Kirchhoff F, Margolis L. 2004. Vpr and Vpu are important
624 for efficient human immunodeficiency virus type 1 replication and CD4+ T-cell depletion
625 in human lymphoid tissue ex vivo. J Virol 78:12689-93.
626 7. Kirchhoff F, Greenough TC, Brettler DB, Sullivan JL, Desrosiers RC. 1995. Brief report:
627 absence of intact nef sequences in a long-term survivor with nonprogressive HIV-1
628 infection. N Engl J Med 332:228-32.
629 8. Haller C, Muller B, Fritz JV, Lamas-Murua M, Stolp B, Pujol FM, Keppler OT, Fackler
630 OT. 2014. HIV-1 Nef and Vpu are functionally redundant broad-spectrum modulators of
631 cell surface receptors, including tetraspanins. J Virol 88:14241-57.
632 9. Tokarev A, Guatelli J. 2011. Misdirection of membrane trafficking by HIV-1 Vpu and Nef:
633 Keys to viral virulence and persistence. Cell Logist 1:90-102.
634 10. Purcell DF, Martin MA. 1993. Alternative splicing of human immunodeficiency virus type
635 1 mRNA modulates viral protein expression, replication, and infectivity. J Virol 67:6365-
636 78.
637 11. Bentham M, Mazaleyrat S, Harris M. 2006. Role of myristoylation and N-terminal basic
638 residues in membrane association of the human immunodeficiency virus type 1 Nef
639 protein. J Gen Virol 87:563-571.
640 12. Craig HM, Reddy TR, Riggs NL, Dao PP, Guatelli JC. 2000. Interactions of HIV-1 nef
641 with the mu subunits of adaptor protein complexes 1, 2, and 3: role of the dileucine-
642 based sorting motif. Virology 271:9-17.
643 13. Chaudhuri R, Lindwasser OW, Smith WJ, Hurley JH, Bonifacino JS. 2007.
644 Downregulation of CD4 by human immunodeficiency virus type 1 Nef is dependent on
645 clathrin and involves direct interaction of Nef with the AP2 clathrin adaptor. J Virol
646 81:3877-90.
647 14. Ren X, Park SY, Bonifacino JS, Hurley JH. 2014. How HIV-1 Nef hijacks the AP-2
648 clathrin adaptor to downregulate CD4. Elife 3:e01754.
649 15. Aiken C, Konner J, Landau NR, Lenburg ME, Trono D. 1994. Nef induces CD4
650 endocytosis: requirement for a critical dileucine motif in the membrane-proximal CD4
651 cytoplasmic domain. Cell 76:853-64.
652 16. Rhee SS, Marsh JW. 1994. Human immunodeficiency virus type 1 Nef-induced down-
653 modulation of CD4 is due to rapid internalization and degradation of surface CD4. J Virol
654 68:5156-63.

655 17. Schwartz S, Felber BK, Pavlakis GN. 1992. Mechanism of translation of monocistronic
656 and multicistronic human immunodeficiency virus type 1 mRNAs. Mol Cell Biol 12:207-
657 19.
658 18. Krummheuer J, Johnson AT, Hauber I, Kammler S, Anderson JL, Hauber J, Purcell DF,
659 Schaal H. 2007. A minimal uORF within the HIV-1 vpu leader allows efficient translation
660 initiation at the downstream env AUG. Virology 363:261-71.
661 19. Wray V, Federau T, Henklein P, Klabunde S, Kunert O, Schomburg D, Schubert U.
662 1995. Solution structure of the hydrophilic region of HIV-1 encoded virus protein U (Vpu)
663 by CD and 1H NMR spectroscopy. Int J Pept Protein Res 45:35-43.
664 20. Maldarelli F, Chen MY, Willey RL, Strebel K. 1993. Human immunodeficiency virus type
665 1 Vpu protein is an oligomeric type I integral membrane protein. J Virol 67:5056-61.
666 21. Marassi FM, Ma C, Gratkowski H, Straus SK, Strebel K, Oblatt-Montal M, Montal M,
667 Opella SJ. 1999. Correlation of the structural and functional domains in the membrane
668 protein Vpu from HIV-1. Proc Natl Acad Sci U S A 96:14336-41.
669 22. Margottin F, Bour SP, Durand H, Selig L, Benichou S, Richard V, Thomas D, Strebel K,
670 Benarous R. 1998. A novel human WD protein, h-beta TrCp, that interacts with HIV-1
671 Vpu connects CD4 to the ER degradation pathway through an F-box motif. Mol Cell
672 1:565-74.
673 23. Coadou G, Evrard-Todeschi N, Gharbi-Benarous J, Benarous R, Girault JP. 2002. HIV-1
674 encoded virus protein U (Vpu) solution structure of the 41-62 hydrophilic region
675 containing the phosphorylated sites Ser52 and Ser56. Int J Biol Macromol 30:23-40.
676 24. Dube M, Roy BB, Guiot-Guillain P, Mercier J, Binette J, Leung G, Cohen EA. 2009.
677 Suppression of Tetherin-restricting activity upon human immunodeficiency virus type 1
678 particle release correlates with localization of Vpu in the trans-Golgi network. J Virol
679 83:4574-90.
680 25. Klimkait T, Strebel K, Hoggan MD, Martin MA, Orenstein JM. 1990. The human
681 immunodeficiency virus type 1-specific protein vpu is required for efficient virus
682 maturation and release. J Virol 64:621-9.
683 26. Schubert U, Strebel K. 1994. Differential activities of the human immunodeficiency virus
684 type 1-encoded Vpu protein are regulated by phosphorylation and occur in different
685 cellular compartments. J Virol 68:2260-71.
686 27. Schubert U, Anton LC, Bacik I, Cox JH, Bour S, Bennink JR, Orlowski M, Strebel K,
687 Yewdell JW. 1998. CD4 glycoprotein degradation induced by human immunodeficiency
688 virus type 1 Vpu protein requires the function of proteasomes and the ubiquitin-
689 conjugating pathway. J Virol 72:2280-8.
690 28. Willey RL, Maldarelli F, Martin MA, Strebel K. 1992. Human immunodeficiency virus type
691 1 Vpu protein induces rapid degradation of CD4. J Virol 66:7193-200.
692 29. Magadan JG, Perez-Victoria FJ, Sougrat R, Ye Y, Strebel K, Bonifacino JS. 2010.
693 Multilayered mechanism of CD4 downregulation by HIV-1 Vpu involving distinct ER
694 retention and ERAD targeting steps. PLoS Pathog 6:e1000869.
695 30. Neil SJ, Zang T, Bieniasz PD. 2008. Tetherin inhibits retrovirus release and is
696 antagonized by HIV-1 Vpu. Nature 451:425-30.
697 31. Van Damme N, Goff D, Katsura C, Jorgenson RL, Mitchell R, Johnson MC, Stephens
698 EB, Guatelli J. 2008. The interferon-induced protein BST-2 restricts HIV-1 release and is
699 downregulated from the cell surface by the viral Vpu protein. Cell Host Microbe 3:245-
700 52.
701 32. Dube M, Roy BB, Guiot-Guillain P, Binette J, Mercier J, Chiasson A, Cohen EA. 2010.
702 Antagonism of tetherin restriction of HIV-1 release by Vpu involves binding and
703 sequestration of the restriction factor in a perinuclear compartment. PLoS Pathog
704 6:e1000856.

705 33. Hauser H, Lopez LA, Yang SJ, Oldenburg JE, Exline CM, Guatelli JC, Cannon PM.
706 2010. HIV-1 Vpu and HIV-2 Env counteract BST-2/tetherin by sequestration in a
707 perinuclear compartment. Retrovirology 7:51.
708 34. Wildum S, Schindler M, Munch J, Kirchhoff F. 2006. Contribution of Vpu, Env, and Nef to
709 CD4 down-modulation and resistance of human immunodeficiency virus type 1-infected
710 T cells to superinfection. J Virol 80:8047-59.
711 35. Ding S, Gasser R, Gendron-Lepage G, Medjahed H, Tolbert WD, Sodroski J, Pazgier M,
712 Finzi A. 2019. CD4 Incorporation into HIV-1 Viral Particles Exposes Envelope Epitopes
713 Recognized by CD4-Induced Antibodies. J Virol 93.
714 36. Bour S, Perrin C, Strebel K. 1999. Cell surface CD4 inhibits HIV-1 particle release by
715 interfering with Vpu activity. J Biol Chem 274:33800-6.
716 37. Cortes MJ, Wong-Staal F, Lama J. 2002. Cell surface CD4 interferes with the infectivity
717 of HIV-1 particles released from T cells. J Biol Chem 277:1770-9.
718 38. Lama J, Mangasarian A, Trono D. 1999. Cell-surface expression of CD4 reduces HIV-1
719 infectivity by blocking Env incorporation in a Nef- and Vpu-inhibitable manner. Curr Biol
720 9:622-31.
721 39. Levesque K, Zhao YS, Cohen EA. 2003. Vpu exerts a positive effect on HIV-1 infectivity
722 by down-modulating CD4 receptor molecules at the surface of HIV-1-producing cells. J
723 Biol Chem 278:28346-53.
724 40. Decker JM, Bibollet-Ruche F, Wei X, Wang S, Levy DN, Wang W, Delaporte E, Peeters
725 M, Derdeyn CA, Allen S, Hunter E, Saag MS, Hoxie JA, Hahn BH, Kwong PD, Robinson
726 JE, Shaw GM. 2005. Antigenic conservation and immunogenicity of the HIV coreceptor
727 binding site. J Exp Med 201:1407-19.
728 41. Veillette M, Coutu M, Richard J, Batraville LA, Dagher O, Bernard N, Tremblay C,
729 Kaufmann DE, Roger M, Finzi A. 2015. The HIV-1 gp120 CD4-Bound Conformation Is
730 Preferentially Targeted by Antibody-Dependent Cellular Cytotoxicity-Mediating
731 Antibodies in Sera from HIV-1-Infected Individuals. J Virol 89:545-51.
732 42. Guan Y, Pazgier M, Sajadi MM, Kamin-Lewis R, Al-Darmarki S, Flinko R, Lovo E, Wu X,
733 Robinson JE, Seaman MS, Fouts TR, Gallo RC, DeVico AL, Lewis GK. 2013. Diverse
734 specificity and effector function among human antibodies to HIV-1 envelope glycoprotein
735 epitopes exposed by CD4 binding. Proc Natl Acad Sci U S A 110:E69-78.
736 43. Veillette M, Desormeaux A, Medjahed H, Gharsallah NE, Coutu M, Baalwa J, Guan Y,
737 Lewis G, Ferrari G, Hahn BH, Haynes BF, Robinson JE, Kaufmann DE, Bonsignori M,
738 Sodroski J, Finzi A. 2014. Interaction with cellular CD4 exposes HIV-1 envelope
739 epitopes targeted by antibody-dependent cell-mediated cytotoxicity. J Virol 88:2633-44.
740 44. Alsahafi N, Ding S, Richard J, Markle T, Brassard N, Walker B, Lewis GK, Kaufmann
741 DE, Brockman MA, Finzi A. 2016. Nef Proteins from HIV-1 Elite Controllers Are
742 Inefficient at Preventing Antibody-Dependent Cellular Cytotoxicity. J Virol 90:2993-3002.
743 45. Schaefer MR, Wonderlich ER, Roeth JF, Leonard JA, Collins KL. 2008. HIV-1 Nef
744 targets MHC-I and CD4 for degradation via a final common beta-COP-dependent
745 pathway in T cells. PLoS Pathog 4:e1000131.
746 46. Dikeakos JD, Atkins KM, Thomas L, Emert-Sedlak L, Byeon IJ, Jung J, Ahn J, Wortman
747 MD, Kukull B, Saito M, Koizumi H, Williamson DM, Hiyoshi M, Barklis E, Takiguchi M,
748 Suzu S, Gronenborn AM, Smithgall TE, Thomas G. 2010. Small molecule inhibition of
749 HIV-1-induced MHC-I down-regulation identifies a temporally regulated switch in Nef
750 action. Mol Biol Cell 21:3279-92.
751 47. Edmonds TG, Ding H, Yuan X, Wei Q, Smith KS, Conway JA, Wieczorek L, Brown B,
752 Polonis V, West JT, Montefiori DC, Kappes JC, Ochsenbauer C. 2010. Replication
753 competent molecular clones of HIV-1 expressing Renilla luciferase facilitate the analysis
754 of antibody inhibition in PBMC. Virology 408:1-13.

755 48. Atkins KM, Thomas L, Youker RT, Harriff MJ, Pissani F, You H, Thomas G. 2008. HIV-1
756 Nef binds PACS-2 to assemble a multikinase cascade that triggers major
757 histocompatibility complex class I (MHC-I) down-regulation: analysis using short
758 interfering RNA and knock-out mice. J Biol Chem 283:11772-84.
759 49. Lenassi M, Cagney G, Liao M, Vaupotic T, Bartholomeeusen K, Cheng Y, Krogan NJ,
760 Plemenitas A, Peterlin BM. 2010. HIV Nef is secreted in exosomes and triggers
761 apoptosis in bystander CD4+ T cells. Traffic 11:110-22.
762 50. Komoto S, Tsuji S, Ibrahim MS, Li YG, Warachit J, Taniguchi K, Ikuta K. 2003. The vpu
763 protein of human immunodeficiency virus type 1 plays a protective role against virus-
764 induced apoptosis in primary CD4(+) T lymphocytes. J Virol 77:10304-13.
765 51. Miyagi E, Andrew AJ, Kao S, Strebel K. 2009. Vpu enhances HIV-1 virus release in the
766 absence of Bst-2 cell surface down-modulation and intracellular depletion. Proc Natl
767 Acad Sci U S A 106:2868-73.
768 52. Chu H, Wang JJ, Qi M, Yoon JJ, Chen X, Wen X, Hammonds J, Ding L, Spearman P.
769 2012. Tetherin/BST-2 is essential for the formation of the intracellular virus-containing
770 compartment in HIV-infected macrophages. Cell Host Microbe 12:360-72.
771 53. Shugars DC, Smith MS, Glueck DH, Nantermet PV, Seillier-Moiseiwitsch F, Swanstrom
772 R. 1993. Analysis of human immunodeficiency virus type 1 nef gene sequences present
773 in vivo. J Virol 67:4639-50.
774 54. Alberti MO, Jones JJ, Miglietta R, Ding H, Bakshi RK, Edmonds TG, Kappes JC,
775 Ochsenbauer C. 2015. Optimized Replicating Renilla Luciferase Reporter HIV-1 Utilizing
776 Novel Internal Ribosome Entry Site Elements for Native Nef Expression and Function.
777 AIDS Res Hum Retroviruses 31:1278-96.
778 55. Jacob RA, Edgar CR, Prevost J, Trothen SM, Lurie A, Mumby MJ, Galbraith A, Kirchhoff
779 F, Haeryfar SMM, Finzi A, Dikeakos JD. 2021. The HIV-1 accessory protein Nef
780 increases surface expression of the checkpoint receptor Tim-3 in infected CD4(+) T
781 cells. J Biol Chem 297:101042.
782 56. Pawlak EN, Dirk BS, Jacob RA, Johnson AL, Dikeakos JD. 2018. The HIV-1 accessory
783 proteins Nef and Vpu downregulate total and cell surface CD28 in CD4(+) T cells.
784 Retrovirology 15:6.
785 57. Cohen EA, Terwilliger EF, Sodroski JG, Haseltine WA. 1988. Identification of a protein
786 encoded by the vpu gene of HIV-1. Nature 334:532-4.
787 58. Heigele A, Kmiec D, Regensburger K, Langer S, Peiffer L, Sturzel CM, Sauter D,
788 Peeters M, Pizzato M, Learn GH, Hahn BH, Kirchhoff F. 2016. The Potency of Nef-
789 Mediated SERINC5 Antagonism Correlates with the Prevalence of Primate Lentiviruses
790 in the Wild. Cell Host Microbe 20:381-91.
791 59. Kmiec D, Iyer SS, Sturzel CM, Sauter D, Hahn BH, Kirchhoff F. 2016. Vpu-Mediated
792 Counteraction of Tetherin Is a Major Determinant of HIV-1 Interferon Resistance. MBio
793 7.
794 60. Bolduan S, Hubel P, Reif T, Lodermeyer V, Hohne K, Fritz JV, Sauter D, Kirchhoff F,
795 Fackler OT, Schindler M, Schubert U. 2013. HIV-1 Vpu affects the anterograde transport
796 and the glycosylation pattern of NTB-A. Virology 440:190-203.
797 61. Bolduan S, Reif T, Schindler M, Schubert U. 2014. HIV-1 Vpu mediated downregulation
798 of CD155 requires alanine residues 10, 14 and 18 of the transmembrane domain.
799 Virology 464-465:375-384.
800 62. Vassena L, Giuliani E, Koppensteiner H, Bolduan S, Schindler M, Doria M. 2015. HIV-1
801 Nef and Vpu Interfere with L-Selectin (CD62L) Cell Surface Expression To Inhibit
802 Adhesion and Signaling in Infected CD4+ T Lymphocytes. J Virol 89:5687-700.
803 63. Prevost J, Pickering S, Mumby MJ, Medjahed H, Gendron-Lepage G, Delgado GG, Dirk
804 BS, Dikeakos JD, Sturzel CM, Sauter D, Kirchhoff F, Bibollet-Ruche F, Hahn BH, Dube
805 M, Kaufmann DE, Neil SJD, Finzi A, Richard J. 2019. Upregulation of BST-2 by Type I

806 Interferons Reduces the Capacity of Vpu To Protect HIV-1-Infected Cells from NK Cell
807 Responses. mBio 10.
808 64. Bour S, Schubert U, Strebel K. 1995. The human immunodeficiency virus type 1 Vpu
809 protein specifically binds to the cytoplasmic domain of CD4: implications for the
810 mechanism of degradation. J Virol 69:1510-20.
811 65. Chen MY, Maldarelli F, Karczewski MK, Willey RL, Strebel K. 1993. Human
812 immunodeficiency virus type 1 Vpu protein induces degradation of CD4 in vitro: the
813 cytoplasmic domain of CD4 contributes to Vpu sensitivity. J Virol 67:3877-84.
814 66. Lenburg ME, Landau NR. 1993. Vpu-induced degradation of CD4: requirement for
815 specific amino acid residues in the cytoplasmic domain of CD4. J Virol 67:7238-45.
816 67. Vincent MJ, Raja NU, Jabbar MA. 1993. Human immunodeficiency virus type 1 Vpu
817 protein induces degradation of chimeric envelope glycoproteins bearing the cytoplasmic
818 and anchor domains of CD4: role of the cytoplasmic domain in Vpu-induced degradation
819 in the endoplasmic reticulum. J Virol 67:5538-49.
820 68. Margottin F, Benichou S, Durand H, Richard V, Liu LX, Gomas E, Benarous R. 1996.
821 Interaction between the cytoplasmic domains of HIV-1 Vpu and CD4: role of Vpu
822 residues involved in CD4 interaction and in vitro CD4 degradation. Virology 223:381-6.
823 69. Prevost J, Edgar CR, Richard J, Trothen SM, Jacob RA, Mumby MJ, Pickering S, Dube
824 M, Kaufmann DE, Kirchhoff F, Neil SJD, Finzi A, Dikeakos JD. 2020. HIV-1 Vpu
825 Downregulates Tim-3 from the Surface of Infected CD4(+) T Cells. J Virol 94.
826 70. Binette J, Dube M, Mercier J, Halawani D, Latterich M, Cohen EA. 2007. Requirements
827 for the selective degradation of CD4 receptor molecules by the human
828 immunodeficiency virus type 1 Vpu protein in the endoplasmic reticulum. Retrovirology
829 4:75.
830 71. Mitchell RS, Katsura C, Skasko MA, Fitzpatrick K, Lau D, Ruiz A, Stephens EB,
831 Margottin-Goguet F, Benarous R, Guatelli JC. 2009. Vpu antagonizes BST-2-mediated
832 restriction of HIV-1 release via beta-TrCP and endo-lysosomal trafficking. PLoS Pathog
833 5:e1000450.
834 72. Gustin JK, Douglas JL, Bai Y, Moses AV. 2012. Ubiquitination of BST-2 protein by HIV-1
835 Vpu protein does not require lysine, serine, or threonine residues within the BST-2
836 cytoplasmic domain. J Biol Chem 287:14837-50.
837 73. Belaidouni N, Marchal C, Benarous R, Besnard-Guerin C. 2007. Involvement of the
838 betaTrCP in the ubiquitination and stability of the HIV-1 Vpu protein. Biochem Biophys
839 Res Commun 357:688-93.
840 74. Kueck T, Neil SJ. 2012. A cytoplasmic tail determinant in HIV-1 Vpu mediates targeting
841 of tetherin for endosomal degradation and counteracts interferon-induced restriction.
842 PLoS Pathog 8:e1002609.
843 75. Kueck T, Foster TL, Weinelt J, Sumner JC, Pickering S, Neil SJ. 2015. Serine
844 Phosphorylation of HIV-1 Vpu and Its Binding to Tetherin Regulates Interaction with
845 Clathrin Adaptors. PLoS Pathog 11:e1005141.
846 76. Mangeat B, Gers-Huber G, Lehmann M, Zufferey M, Luban J, Piguet V. 2009. HIV-1 Vpu
847 neutralizes the antiviral factor Tetherin/BST-2 by binding it and directing its beta-TrCP2-
848 dependent degradation. PLoS Pathog 5:e1000574.
849 77. Arias JF, Heyer LN, von Bredow B, Weisgrau KL, Moldt B, Burton DR, Rakasz EG,
850 Evans DT. 2014. Tetherin antagonism by Vpu protects HIV-infected cells from antibody-
851 dependent cell-mediated cytotoxicity. Proc Natl Acad Sci U S A 111:6425-30.
852 78. Alvarez RA, Hamlin RE, Monroe A, Moldt B, Hotta MT, Rodriguez Caprio G, Fierer DS,
853 Simon V, Chen BK. 2014. HIV-1 Vpu antagonism of tetherin inhibits antibody-dependent
854 cellular cytotoxic responses by natural killer cells. J Virol 88:6031-46.

855 79. Prevost J, Richard J, Medjahed H, Alexander A, Jones J, Kappes JC, Ochsenbauer C,
856 Finzi A. 2018. Incomplete Downregulation of CD4 Expression Affects HIV-1 Env
857 Conformation and Antibody-Dependent Cellular Cytotoxicity Responses. J Virol 92.
858 80. Ding S, Veillette M, Coutu M, Prevost J, Scharf L, Bjorkman PJ, Ferrari G, Robinson JE,
859 Sturzel C, Hahn BH, Sauter D, Kirchhoff F, Lewis GK, Pazgier M, Finzi A. 2016. A Highly
860 Conserved Residue of the HIV-1 gp120 Inner Domain Is Important for Antibody-
861 Dependent Cellular Cytotoxicity Responses Mediated by Anti-cluster A Antibodies. J
862 Virol 90:2127-34.
863 81. Ferrari G, Pollara J, Kozink D, Harms T, Drinker M, Freel S, Moody MA, Alam SM,
864 Tomaras GD, Ochsenbauer C, Kappes JC, Shaw GM, Hoxie JA, Robinson JE, Haynes
865 BF. 2011. An HIV-1 gp120 envelope human monoclonal antibody that recognizes a C1
866 conformational epitope mediates potent antibody-dependent cellular cytotoxicity (ADCC)
867 activity and defines a common ADCC epitope in human HIV-1 serum. J Virol 85:7029-
868 36.
869 82. Tomaras GD, Ferrari G, Shen X, Alam SM, Liao HX, Pollara J, Bonsignori M, Moody
870 MA, Fong Y, Chen X, Poling B, Nicholson CO, Zhang R, Lu X, Parks R, Kaewkungwal J,
871 Nitayaphan S, Pitisuttithum P, Rerks-Ngarm S, Gilbert PB, Kim JH, Michael NL,
872 Montefiori DC, Haynes BF. 2013. Vaccine-induced plasma IgA specific for the C1 region
873 of the HIV-1 envelope blocks binding and effector function of IgG. Proc Natl Acad Sci U
874 S A doi:10.1073/pnas.1301456110.
875 83. Pollara J, Bonsignori M, Moody MA, Liu P, Alam SM, Hwang KK, Gurley TC, Kozink DM,
876 Armand LC, Marshall DJ, Whitesides JF, Kaewkungwal J, Nitayaphan S, Pitisuttithum P,
877 Rerks-Ngarm S, Robb ML, O'Connell RJ, Kim JH, Michael NL, Montefiori DC, Tomaras
878 GD, Liao HX, Haynes BF, Ferrari G. 2014. HIV-1 vaccine-induced C1 and V2 Env-
879 specific antibodies synergize for increased antiviral activities. J Virol 88:7715-26.
880 84. Santra S, Tomaras GD, Warrier R, Nicely NI, Liao HX, Pollara J, Liu P, Alam SM, Zhang
881 R, Cocklin SL, Shen X, Duffy R, Xia SM, Schutte RJ, Pemble Iv CW, Dennison SM, Li H,
882 Chao A, Vidnovic K, Evans A, Klein K, Kumar A, Robinson J, Landucci G, Forthal DN,
883 Montefiori DC, Kaewkungwal J, Nitayaphan S, Pitisuttithum P, Rerks-Ngarm S, Robb
884 ML, Michael NL, Kim JH, Soderberg KA, Giorgi EE, Blair L, Korber BT, Moog C,
885 Shattock RJ, Letvin NL, Schmitz JE, Moody MA, Gao F, Ferrari G, Shaw GM, Haynes
886 BF. 2015. Human Non-neutralizing HIV-1 Envelope Monoclonal Antibodies Limit the
887 Number of Founder Viruses during SHIV Mucosal Infection in Rhesus Macaques. PLoS
888 Pathog 11:e1005042.
889 85. Huang Y, Ferrari G, Alter G, Forthal DN, Kappes JC, Lewis GK, Love JC, Borate B,
890 Harris L, Greene K, Gao H, Phan TB, Landucci G, Goods BA, Dowell KG, Cheng HD,
891 Bailey-Kellogg C, Montefiori DC, Ackerman ME. 2016. Diversity of Antiviral IgG Effector
892 Activities Observed in HIV-Infected and Vaccinated Subjects. J Immunol 197:4603-4612.
893 86. Costa MR, Pollara J, Edwards RW, Seaman MS, Gorny MK, Montefiori DC, Liao HX,
894 Ferrari G, Lu S, Wang S. 2016. Fc Receptor-Mediated Activities of Env-Specific Human
895 Monoclonal Antibodies Generated from Volunteers Receiving the DNA Prime-Protein
896 Boost HIV Vaccine DP6-001. J Virol 90:10362-10378.
897 87. Bradley T, Pollara J, Santra S, Vandergrift N, Pittala S, Bailey-Kellogg C, Shen X, Parks
898 R, Goodman D, Eaton A, Balachandran H, Mach LV, Saunders KO, Weiner JA, Scearce
899 R, Sutherland LL, Phogat S, Tartaglia J, Reed SG, Hu SL, Theis JF, Pinter A, Montefiori
900 DC, Kepler TB, Peachman KK, Rao M, Michael NL, Suscovich TJ, Alter G, Ackerman
901 ME, Moody MA, Liao HX, Tomaras G, Ferrari G, Korber BT, Haynes BF. 2017.
902 Pentavalent HIV-1 vaccine protects against simian-human immunodeficiency virus
903 challenge. Nat Commun 8:15711.
904 88. Meyerhoff RR, Scearce RM, Ogburn DF, Lockwood B, Pickeral J, Kuraoka M, Anasti K,
905 Eudailey J, Eaton A, Cooper M, Wiehe K, Montefiori DC, Tomaras G, Ferrari G, Alam

906 SM, Liao HX, Korber B, Gao F, Haynes BF. 2017. HIV-1 Consensus Envelope-Induced
907 Broadly Binding Antibodies. AIDS Res Hum Retroviruses 33:859-868.
908 89. Sung JA, Pickeral J, Liu L, Stanfield-Oakley SA, Lam CK, Garrido C, Pollara J,
909 LaBranche C, Bonsignori M, Moody MA, Yang Y, Parks R, Archin N, Allard B, Kirchherr
910 J, Kuruc JD, Gay CL, Cohen MS, Ochsenbauer C, Soderberg K, Liao HX, Montefiori D,
911 Moore P, Johnson S, Koenig S, Haynes BF, Nordstrom JL, Margolis DM, Ferrari G.
912 2015. Dual-Affinity Re-Targeting proteins direct T cell-mediated cytolysis of latently HIV-
913 infected cells. J Clin Invest doi:10.1172/JCI82314.
914 90. Tuyishime M, Garrido C, Jha S, Moeser M, Mielke D, LaBranche C, Montefiori D,
915 Haynes BF, Joseph S, Margolis DM, Ferrari G. 2020. Improved killing of HIV-infected
916 cells using three neutralizing and non-neutralizing antibodies. J Clin Invest 130:5157-
917 5170.
918 91. Bonsignori M, Pollara J, Moody MA, Alpert MD, Chen X, Hwang KK, Gilbert PB, Huang
919 Y, Gurley TC, Kozink DM, Marshall DJ, Whitesides JF, Tsao CY, Kaewkungwal J,
920 Nitayaphan S, Pitisuttithum P, Rerks-Ngarm S, Kim JH, Michael NL, Tomaras GD,
921 Montefiori DC, Lewis GK, Devico A, Evans DT, Ferrari G, Liao HX, Haynes BF. 2012.
922 Antibody-Dependent Cellular Cytotoxicity-Mediating Antibodies from an HIV-1 Vaccine
923 Efficacy Trial Target Multiple Epitopes and Preferentially Use the VH1 Gene Family. J
924 Virol 86:11521-32.
925 92. Cheng HD, Dowell KG, Bailey-Kellogg C, Goods BA, Love JC, Ferrari G, Alter G, Gach
926 J, Forthal DN, Lewis GK, Greene K, Gao H, Montefiori DC, Ackerman ME. 2021. Diverse
927 antiviral IgG effector activities are predicted by unique biophysical antibody features.
928 Retrovirology 18:35.
929 93. Pollara J, Jones DI, Huffman T, Edwards RW, Dennis M, Li SH, Jha S, Goodman D,
930 Kumar A, LaBranche CC, Montefiori DC, Fouda GG, Hope TJ, Tomaras GD, Staats HF,
931 Ferrari G, Permar SR. 2019. Bridging Vaccine-Induced HIV-1 Neutralizing and Effector
932 Antibody Responses in Rabbit and Rhesus Macaque Animal Models. J Virol 93.
933 94. Fisher L, Zinter M, Stanfield-Oakley S, Carpp LN, Edwards RW, Denny T, Moodie Z,
934 Laher F, Bekker LG, McElrath MJ, Gilbert PB, Corey L, Tomaras G, Pollara J, Ferrari G.
935 2019. Vaccine-Induced Antibodies Mediate Higher Antibody-Dependent Cellular
936 Cytotoxicity After Interleukin-15 Pretreatment of Natural Killer Effector Cells. Front
937 Immunol 10:2741.
938 95. Lewis GK, Ackerman ME, Scarlatti G, Moog C, Robert-Guroff M, Kent SJ, Overbaugh J,
939 Reeves RK, Ferrari G, Thyagarajan B. 2019. Knowns and Unknowns of Assaying
940 Antibody-Dependent Cell-Mediated Cytotoxicity Against HIV-1. Front Immunol 10:1025.
941 96. Easterhoff D, Pollara J, Luo K, Tolbert WD, Young B, Mielke D, Jha S, O'Connell RJ,
942 Vasan S, Kim J, Michael NL, Excler JL, Robb ML, Rerks-Ngarm S, Kaewkungwal J,
943 Pitisuttithum P, Nitayaphan S, Sinangil F, Tartaglia J, Phogat S, Kepler TB, Alam SM,
944 Wiehe K, Saunders KO, Montefiori DC, Tomaras GD, Moody MA, Pazgier M, Haynes
945 BF, Ferrari G. 2020. Boosting with AIDSVAX B/E Enhances Env Constant Region 1 and
946 2 Antibody-Dependent Cellular Cytotoxicity Breadth and Potency. J Virol 94.
947 97. Tolbert WD, Van V, Sherburn R, Tuyishime M, Yan F, Nguyen DN, Stanfield-Oakley S,
948 Easterhoff D, Bonsignori M, Haynes BF, Moody MA, Ray K, Ferrari G, Lewis GK,
949 Pazgier M. 2020. Recognition Patterns of the C1/C2 Epitopes Involved in Fc-Mediated
950 Response in HIV-1 Natural Infection and the RV114 Vaccine Trial. mBio 11.
951 98. Madani N, Princiotto AM, Mach L, Ding S, Prevost J, Richard J, Hora B, Sutherland L,
952 Zhao CA, Conn BP, Bradley T, Moody MA, Melillo B, Finzi A, Haynes BF, Smith AB, III,
953 Santra S, Sodroski J. 2018. A CD4-mimetic compound enhances vaccine efficacy
954 against stringent immunodeficiency virus challenge. Nat Commun 9:2363.
955 99. Strebel K. 2013. HIV accessory proteins versus host restriction factors. Curr Opin Virol
956 3:692-9.

957 100. Ramirez PW, Famiglietti M, Sowrirajan B, DePaula-Silva AB, Rodesch C, Barker E,
958 Bosque A, Planelles V. 2014. Downmodulation of CCR7 by HIV-1 Vpu results in
959 impaired migration and chemotactic signaling within CD4(+) T cells. Cell Rep 7:2019-30.
960 101. Usami Y, Wu Y, Gottlinger HG. 2015. SERINC3 and SERINC5 restrict HIV-1 infectivity
961 and are counteracted by Nef. Nature 526:218-23.
962 102. Rosa A, Chande A, Ziglio S, De Sanctis V, Bertorelli R, Goh SL, McCauley SM,
963 Nowosielska A, Antonarakis SE, Luban J, Santoni FA, Pizzato M. 2015. HIV-1 Nef
964 promotes infection by excluding SERINC5 from virion incorporation. Nature 526:212-7.
965 103. Liu Y, Fu Y, Wang Q, Li M, Zhou Z, Dabbagh D, Fu C, Zhang H, Li S, Zhang T, Gong J,
966 Kong X, Zhai W, Su J, Sun J, Zhang Y, Yu XF, Shao Z, Zhou F, Wu Y, Tan X. 2019.
967 Proteomic profiling of HIV-1 infection of human CD4(+) T cells identifies PSGL-1 as an
968 HIV restriction factor. Nat Microbiol 4:813-825.
969 104. Fu Y, He S, Waheed AA, Dabbagh D, Zhou Z, Trinite B, Wang Z, Yu J, Wang D, Li F,
970 Levy DN, Shang H, Freed EO, Wu Y. 2020. PSGL-1 restricts HIV-1 infectivity by
971 blocking virus particle attachment to target cells. Proc Natl Acad Sci U S A 117:9537-
972 9545.
973 105. Schwartz O, Marechal V, Le Gall S, Lemonnier F, Heard JM. 1996. Endocytosis of major
974 histocompatibility complex class I molecules is induced by the HIV-1 Nef protein. Nat
975 Med 2:338-42.
976 106. Collins KL, Chen BK, Kalams SA, Walker BD, Baltimore D. 1998. HIV-1 Nef protein
977 protects infected primary cells against killing by cytotoxic T lymphocytes. Nature
978 391:397-401.
979 107. Cerboni C, Neri F, Casartelli N, Zingoni A, Cosman D, Rossi P, Santoni A, Doria M.
980 2007. Human immunodeficiency virus 1 Nef protein downmodulates the ligands of the
981 activating receptor NKG2D and inhibits natural killer cell-mediated cytotoxicity. J Gen
982 Virol 88:242-50.
983 108. Fausther-Bovendo H, Sol-Foulon N, Candotti D, Agut H, Schwartz O, Debre P, Vieillard
984 V. 2009. HIV escape from natural killer cytotoxicity: nef inhibits NKp44L expression on
985 CD4+ T cells. AIDS 23:1077-87.
986 109. Shah AH, Sowrirajan B, Davis ZB, Ward JP, Campbell EM, Planelles V, Barker E. 2010.
987 Degranulation of natural killer cells following interaction with HIV-1-infected cells is
988 hindered by downmodulation of NTB-A by Vpu. Cell Host Microbe 8:397-409.
989 110. Matusali G, Potesta M, Santoni A, Cerboni C, Doria M. 2012. The human
990 immunodeficiency virus type 1 Nef and Vpu proteins downregulate the natural killer cell-
991 activating ligand PVR. J Virol 86:4496-504.
992 111. Apps R, Del Prete GQ, Chatterjee P, Lara A, Brumme ZL, Brockman MA, Neil S,
993 Pickering S, Schneider DK, Piechocka-Trocha A, Walker BD, Thomas R, Shaw GM,
994 Hahn BH, Keele BF, Lifson JD, Carrington M. 2016. HIV-1 Vpu Mediates HLA-C
995 Downregulation. Cell Host Microbe 19:686-95.
996 112. Moll M, Andersson SK, Smed-Sorensen A, Sandberg JK. 2010. Inhibition of lipid antigen
997 presentation in dendritic cells by HIV-1 Vpu interference with CD1d recycling from
998 endosomal compartments. Blood 116:1876-84.
999 113. Chen N, McCarthy C, Drakesmith H, Li D, Cerundolo V, McMichael AJ, Screaton GR, Xu
1000 XN. 2006. HIV-1 down-regulates the expression of CD1d via Nef. Eur J Immunol 36:278-
1001 86.
1002 114. Pacyniak E, Gomez ML, Gomez LM, Mulcahy ER, Jackson M, Hout DR, Wisdom BJ,
1003 Stephens EB. 2005. Identification of a region within the cytoplasmic domain of the
1004 subtype B Vpu protein of human immunodeficiency virus type 1 (HIV-1) that is
1005 responsible for retention in the golgi complex and its absence in the Vpu protein from a
1006 subtype C HIV-1. AIDS Res Hum Retroviruses 21:379-94.

1007 115. Pickering S, Hue S, Kim EY, Reddy S, Wolinsky SM, Neil SJ. 2014. Preservation of
1008 Tetherin and CD4 Counter-Activities in Circulating Vpu Alleles despite Extensive
1009 Sequence Variation within HIV-1 Infected Individuals. PLoS Pathog 10:e1003895.
1010 116. Iwami S, Sato K, Morita S, Inaba H, Kobayashi T, Takeuchi JS, Kimura Y, Misawa N,
1011 Ren F, Iwasa Y, Aihara K, Koyanagi Y. 2015. Pandemic HIV-1 Vpu overcomes intrinsic
1012 herd immunity mediated by tetherin. Sci Rep 5:12256.
1013 117. Chen BK, Gandhi RT, Baltimore D. 1996. CD4 down-modulation during infection of
1014 human T cells with human immunodeficiency virus type 1 involves independent activities
1015 of vpu, env, and nef. J Virol 70:6044-53.
1016 118. Richard J, Veillette M, Brassard N, Iyer SS, Roger M, Martin L, Pazgier M, Schon A,
1017 Freire E, Routy JP, Smith AB, III, Park J, Jones DM, Courter JR, Melillo BN, Kaufmann
1018 DE, Hahn BH, Permar SR, Haynes BF, Madani N, Sodroski JG, Finzi A. 2015. CD4
1019 mimetics sensitize HIV-1-infected cells to ADCC. Proc Natl Acad Sci U S A 112:E2687-
1020 94.
1021 119. Prevost J, Zoubchenok D, Richard J, Veillette M, Pacheco B, Coutu M, Brassard N,
1022 Parsons MS, Ruxrungtham K, Bunupuradah T, Tovanabutra S, Hwang KK, Moody MA,
1023 Haynes BF, Bonsignori M, Sodroski J, Kaufmann DE, Shaw GM, Chenine AL, Finzi A.
1024 2017. Influence of the Envelope gp120 Phe 43 Cavity on HIV-1 Sensitivity to Antibody-
1025 Dependent Cell-Mediated Cytotoxicity Responses. J Virol 91.
1026 120. Prevost J, Richard J, Ding S, Pacheco B, Charlebois R, Hahn BH, Kaufmann DE, Finzi
1027 A. 2018. Envelope glycoproteins sampling states 2/3 are susceptible to ADCC by sera
1028 from HIV-1-infected individuals. Virology 515:38-45.
1029 121. Richard J, Prevost J, von Bredow B, Ding S, Brassard N, Medjahed H, Coutu M, Melillo
1030 B, Bibollet-Ruche F, Hahn BH, Kaufmann DE, Smith AB, 3rd, Sodroski J, Sauter D,
1031 Kirchhoff F, Gee K, Neil SJ, Evans DT, Finzi A. 2017. BST-2 Expression Modulates
1032 Small CD4-Mimetic Sensitization of HIV-1-Infected Cells to Antibody-Dependent Cellular
1033 Cytotoxicity. J Virol 91.
1034 122. Richard J, Prevost J, Alsahafi N, Ding S, Finzi A. 2018. Impact of HIV-1 Envelope
1035 Conformation on ADCC Responses. Trends Microbiol 26:253-265.
1036 123. Alpert MD, Heyer LN, Williams DE, Harvey JD, Greenough T, Allhorn M, Evans DT.
1037 2012. A novel assay for antibody-dependent cell-mediated cytotoxicity against HIV-1- or
1038 SIV-infected cells reveals incomplete overlap with antibodies measured by neutralization
1039 and binding assays. J Virol 86:12039-52.
1040 124. Fontaine J, Chagnon-Choquet J, Valcke HS, Poudrier J, Roger M. 2011. High
1041 expression levels of B lymphocyte stimulator (BLyS) by dendritic cells correlate with HIV-
1042 related B-cell disease progression in humans. Blood 117:145-55.
1043 125. Fontaine J, Coutlee F, Tremblay C, Routy JP, Poudrier J, Roger M. 2009. HIV infection
1044 affects blood myeloid dendritic cells after successful therapy and despite nonprogressing
1045 clinical disease. J Infect Dis 199:1007-18.
1046 126. International HIVCS, Pereyra F, Jia X, McLaren PJ, Telenti A, de Bakker PI, Walker BD,
1047 Ripke S, Brumme CJ, Pulit SL, Carrington M, Kadie CM, Carlson JM, Heckerman D,
1048 Graham RR, Plenge RM, Deeks SG, Gianniny L, Crawford G, Sullivan J, Gonzalez E,
1049 Davies L, Camargo A, Moore JM, Beattie N, Gupta S, Crenshaw A, Burtt NP, Guiducci
1050 C, Gupta N, Gao X, Qi Y, Yuki Y, Piechocka-Trocha A, Cutrell E, Rosenberg R, Moss
1051 KL, Lemay P, O'Leary J, Schaefer T, Verma P, Toth I, Block B, Baker B, Rothchild A,
1052 Lian J, Proudfoot J, Alvino DM, Vine S, Addo MM, et al. 2010. The major genetic
1053 determinants of HIV-1 control affect HLA class I peptide presentation. Science
1054 330:1551-7.
1055 127. Kamya P, Boulet S, Tsoukas CM, Routy JP, Thomas R, Cote P, Boulassel MR, Baril JG,
1056 Kovacs C, Migueles SA, Connors M, Suscovich TJ, Brander C, Tremblay CL, Bernard N.
1057 2011. Receptor-ligand requirements for increased NK cell polyfunctional potential in slow

1058 progressors infected with HIV-1 coexpressing KIR3DL1*h/*y and HLA-B*57. J Virol
1059 85:5949-60.
1060 128. Peretz Y, Ndongala ML, Boulet S, Boulassel MR, Rouleau D, Cote P, Longpre D, Routy
1061 JP, Falutz J, Tremblay C, Tsoukas CM, Sekaly RP, Bernard NF. 2007. Functional T cell
1062 subsets contribute differentially to HIV peptide-specific responses within infected
1063 individuals: correlation of these functional T cell subsets with markers of disease
1064 progression. Clin Immunol 124:57-68.
1065 129. Finzi A, Xiang SH, Pacheco B, Wang L, Haight J, Kassa A, Danek B, Pancera M, Kwong
1066 PD, Sodroski J. 2010. Topological layers in the HIV-1 gp120 inner domain regulate gp41
1067 interaction and CD4-triggered conformational transitions. Mol Cell 37:656-67.
1068 130. Emi N, Friedmann T, Yee JK. 1991. Pseudotype formation of murine leukemia virus with
1069 the G protein of vesicular stomatitis virus. J Virol 65:1202-7.
1070 131. Salazar-Gonzalez JF, Salazar MG, Keele BF, Learn GH, Giorgi EE, Li H, Decker JM,
1071 Wang S, Baalwa J, Kraus MH, Parrish NF, Shaw KS, Guffey MB, Bar KJ, Davis KL,
1072 Ochsenbauer-Jambor C, Kappes JC, Saag MS, Cohen MS, Mulenga J, Derdeyn CA,
1073 Allen S, Hunter E, Markowitz M, Hraber P, Perelson AS, Bhattacharya T, Haynes BF,
1074 Korber BT, Hahn BH, Shaw GM. 2009. Genetic identity, biological phenotype, and
1075 evolutionary pathways of transmitted/founder viruses in acute and early HIV-1 infection.
1076 J Exp Med 206:1273-89.
1077 132. Ochsenbauer C, Edmonds TG, Ding H, Keele BF, Decker J, Salazar MG, Salazar-
1078 Gonzalez JF, Shattock R, Haynes BF, Shaw GM, Hahn BH, Kappes JC. 2012.
1079 Generation of Transmitted/Founder HIV-1 Infectious Molecular Clones and
1080 Characterization of Their Replication Capacity in CD4 T Lymphocytes and Monocyte-
1081 Derived Macrophages. J Virol 86:2715-28.
1082 133. Parrish NF, Wilen CB, Banks LB, Iyer SS, Pfaff JM, Salazar-Gonzalez JF, Salazar MG,
1083 Decker JM, Parrish EH, Berg A, Hopper J, Hora B, Kumar A, Mahlokozera T, Yuan S,
1084 Coleman C, Vermeulen M, Ding H, Ochsenbauer C, Tilton JC, Permar SR, Kappes JC,
1085 Betts MR, Busch MP, Gao F, Montefiori D, Haynes BF, Shaw GM, Hahn BH, Doms RW.
1086 2012. Transmitted/founder and chronic subtype C HIV-1 use CD4 and CCR5 receptors
1087 with equal efficiency and are not inhibited by blocking the integrin alpha4beta7. PLoS
1088 Pathog 8:e1002686.
1089 134. Parrish NF, Gao F, Li H, Giorgi EE, Barbian HJ, Parrish EH, Zajic L, Iyer SS, Decker JM,
1090 Kumar A, Hora B, Berg A, Cai F, Hopper J, Denny TN, Ding H, Ochsenbauer C, Kappes
1091 JC, Galimidi RP, West AP, Jr., Bjorkman PJ, Wilen CB, Doms RW, O'Brien M, Bhardwaj
1092 N, Borrow P, Haynes BF, Muldoon M, Theiler JP, Korber B, Shaw GM, Hahn BH. 2013.
1093 Phenotypic properties of transmitted founder HIV-1. Proc Natl Acad Sci U S A 110:6626-
1094 33.
1095 135. Fenton-May AE, Dibben O, Emmerich T, Ding H, Pfafferott K, Aasa-Chapman MM,
1096 Pellegrino P, Williams I, Cohen MS, Gao F, Shaw GM, Hahn BH, Ochsenbauer C,
1097 Kappes JC, Borrow P. 2013. Relative resistance of HIV-1 founder viruses to control by
1098 interferon-alpha. Retrovirology 10:146.
1099 136. Liao HX, Lynch R, Zhou T, Gao F, Alam SM, Boyd SD, Fire AZ, Roskin KM, Schramm
1100 CA, Zhang Z, Zhu J, Shapiro L, Mullikin JC, Gnanakaran S, Hraber P, Wiehe K, Kelsoe
1101 G, Yang G, Xia SM, Montefiori DC, Parks R, Lloyd KE, Scearce RM, Soderberg KA,
1102 Cohen M, Kamanga G, Louder MK, Tran LM, Chen Y, Cai F, Chen S, Moquin S, Du X,
1103 Joyce MG, Srivatsan S, Zhang B, Zheng A, Shaw GM, Hahn BH, Kepler TB, Korber BT,
1104 Kwong PD, Mascola JR, Haynes BF. 2013. Co-evolution of a broadly neutralizing HIV-1
1105 antibody and founder virus. Nature 496:469-76.
1106 137. Gao F, Bonsignori M, Liao HX, Kumar A, Xia SM, Lu X, Cai F, Hwang KK, Song H, Zhou
1107 T, Lynch RM, Alam SM, Moody MA, Ferrari G, Berrong M, Kelsoe G, Shaw GM, Hahn
1108 BH, Montefiori DC, Kamanga G, Cohen MS, Hraber P, Kwong PD, Korber BT, Mascola

1109 JR, Kepler TB, Haynes BF. 2014. Cooperation of B cell lineages in induction of HIV-1-
1110 broadly neutralizing antibodies. Cell 158:481-91.
1111 138. Salminen MO, Ehrenberg PK, Mascola JR, Dayhoff DE, Merling R, Blake B, Louder M,
1112 Hegerich S, Polonis VR, Birx DL, Robb ML, McCutchan FE, Michael NL. 2000.
1113 Construction and biological characterization of infectious molecular clones of HIV-1
1114 subtypes B and E (CRF01_AE) generated by the polymerase chain reaction. Virology
1115 278:103-10.
1116 139. Chenine AL, Merbah M, Wieczorek L, Molnar S, Mann B, Lee J, O'Sullivan AM, Bose M,
1117 Sanders-Buell E, Kijak GH, Herrera C, McLinden R, O'Connell RJ, Michael NL, Robb
1118 ML, Kim JH, Polonis VR, Tovanabutra S. 2018. Neutralization Sensitivity of a Novel HIV-
1119 1 CRF01_AE Panel of Infectious Molecular Clones. J Acquir Immune Defic Syndr
1120 78:348-355.
1121 140. Peachman KK, Karasavvas N, Chenine AL, McLinden R, Rerks-Ngarm S, Jaranit K,
1122 Nitayaphan S, Pitisuttithum P, Tovanabutra S, Zolla-Pazner S, Michael NL, Kim JH,
1123 Alving CR, Rao M. 2015. Identification of New Regions in HIV-1 gp120 Variable 2 and 3
1124 Loops that Bind to alpha4beta7 Integrin Receptor. PLoS One 10:e0143895.
1125 141. O'Brien WA, Koyanagi Y, Namazie A, Zhao JQ, Diagne A, Idler K, Zack JA, Chen IS.
1126 1990. HIV-1 tropism for mononuclear phagocytes can be determined by regions of
1127 gp120 outside the CD4-binding domain. Nature 348:69-73.
1128 142. Li Y, Kappes JC, Conway JA, Price RW, Shaw GM, Hahn BH. 1991. Molecular
1129 characterization of human immunodeficiency virus type 1 cloned directly from uncultured
1130 human brain tissue: identification of replication-competent and -defective viral genomes.
1131 J Virol 65:3973-85.
1132 143. Theodore TS, Englund G, Buckler-White A, Buckler CE, Martin MA, Peden KW. 1996.
1133 Construction and characterization of a stable full-length macrophage-tropic HIV type 1
1134 molecular clone that directs the production of high titers of progeny virions. AIDS Res
1135 Hum Retroviruses 12:191-4.
1136 144. Krapp C, Hotter D, Gawanbacht A, McLaren PJ, Kluge SF, Sturzel CM, Mack K, Reith E,
1137 Engelhart S, Ciuffi A, Hornung V, Sauter D, Telenti A, Kirchhoff F. 2016. Guanylate
1138 Binding Protein (GBP) 5 Is an Interferon-Inducible Inhibitor of HIV-1 Infectivity. Cell Host
1139 Microbe 19:504-14.
1140 145. Koyanagi Y, Miles S, Mitsuyasu RT, Merrill JE, Vinters HV, Chen IS. 1987. Dual infection
1141 of the central nervous system by AIDS viruses with distinct cellular tropisms. Science
1142 236:819-22.
1143 146. Adachi A, Gendelman HE, Koenig S, Folks T, Willey R, Rabson A, Martin MA. 1986.
1144 Production of acquired immunodeficiency syndrome-associated retrovirus in human and
1145 nonhuman cells transfected with an infectious molecular clone. J Virol 59:284-91.
1146 147. Mack K, Starz K, Sauter D, Langer S, Bibollet-Ruche F, Learn GH, Sturzel CM, Leoz M,
1147 Plantier JC, Geyer M, Hahn BH, Kirchhoff F. 2017. Efficient Vpu-Mediated Tetherin
1148 Antagonism by an HIV-1 Group O Strain. J Virol 91.
1149 148. Takehisa J, Kraus MH, Decker JM, Li Y, Keele BF, Bibollet-Ruche F, Zammit KP, Weng
1150 Z, Santiago ML, Kamenya S, Wilson ML, Pusey AE, Bailes E, Sharp PM, Shaw GM,
1151 Hahn BH. 2007. Generation of infectious molecular clones of simian immunodeficiency
1152 virus from fecal consensus sequences of wild chimpanzees. J Virol 81:7463-75.
1153 149. Shingai M, Donau OK, Schmidt SD, Gautam R, Plishka RJ, Buckler-White A,
1154 Sadjadpour R, Lee WR, LaBranche CC, Montefiori DC, Mascola JR, Nishimura Y, Martin
1155 MA. 2012. Most rhesus macaques infected with the CCR5-tropic SHIV(AD8) generate
1156 cross-reactive antibodies that neutralize multiple HIV-1 strains. Proc Natl Acad Sci U S A
1157 109:19769-74.
1158 150. Li H, Wang S, Lee FH, Roark RS, Murphy AI, Smith J, Zhao C, Rando J, Chohan N,
1159 Ding Y, Kim E, Lindemuth E, Bar KJ, Pandrea I, Apetrei C, Keele BF, Lifson JD, Lewis

1160 MG, Denny TN, Haynes BF, Hahn BH, Shaw GM. 2021. New SHIVs and Improved
1161 Design Strategy for Modeling HIV-1 Transmission, Immunopathogenesis, Prevention
1162 and Cure. J Virol doi:10.1128/JVI.00071-21.
1163 151. R Core Team. 2013. R: A language and environment for statistical computing, R
1164 Foundation for Statistical Computing, Vienna, Austria. https://www.R-project.org/.
1165 152. RStudio team. 2015. RStudio: Integrated Development for R, RStudio, Inc., Boston, MA.
1166 http://www.rstudio.com/.
1167 153. Crooks GE, Hon G, Chandonia JM, Brenner SE. 2004. WebLogo: a sequence logo
1168 generator. Genome Res 14:1188-90.

1169

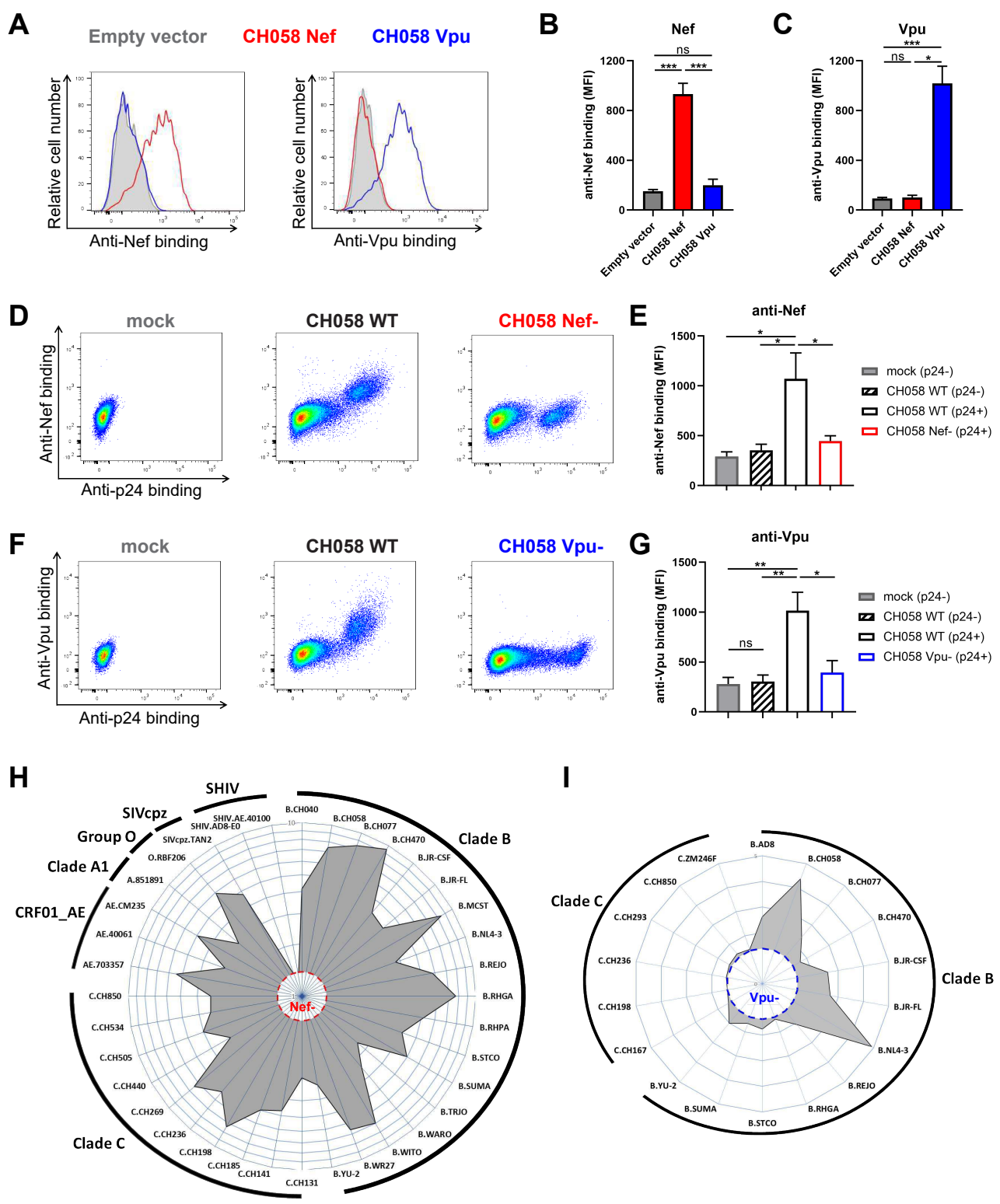

Figure 1. Intracellular detection of Nef and Vpu in infected primary CD4+ T cells.
(**A-C**) 293T cells transfected with an empty vector or a plasmid expressing either CH058 Nef or CH058 Vpu. 48 hours post-transfection, cells were permeabilized and stained with rabbit polyclonal antisera raised against Nef and Vpu to detect their respective intracellular expression. Antiserum binding was detected using donkey anti-rabbit BV421 secondary Abs. (**A**) Histograms depicting representative staining and (**B-C**) Median fluorescence intensities (MFI) obtained for multiple independent stainings using (**B**) anti-Nef or (**C**) anti-Vpu. (**D-G**) Primary CD4+T cells mock-infected or infected with CH058 T/F WT, Nef- or Vpu-, were stained to detect the intracellular expression of Nef or Vpu. (**D,F**) Dot plots (left) and histograms (right) depicting representative (**D**) Nef and (**F**) Vpu staining. (**E,G**) The graphs show the MFI obtained from different cell populations using cells from five different donors using (**E**) anti-Nef or (**G**) anti-Vpu. Error bars indicate means ± standard errors of the means (SEM). Statistical significance was tested using an unpaired t test or a Mann-Whitney U test based on statistical normality (*, P<0.05; **, P<0.01; ***, P<0.001; ns, nonsignificant). (**H-I**) Primary CD4+ T cells were infected with a panel of viruses from different clades (A1, B, C, CRF01_AE), group (M, O) and host (HIV-1, SIVcpz, SHIV). The radar plots indicate the level of specific recognition of infected cells (MFI normalized to uninfected cells) using the (**H**) anti-Nef or (**I**) anti-Vpu antisera. The limit of detection was determined using (**H**) cells infected with CH058 Nef- for Nef staining and using (**I**) cells infected with CH058 Vpu- for Vpu staining.

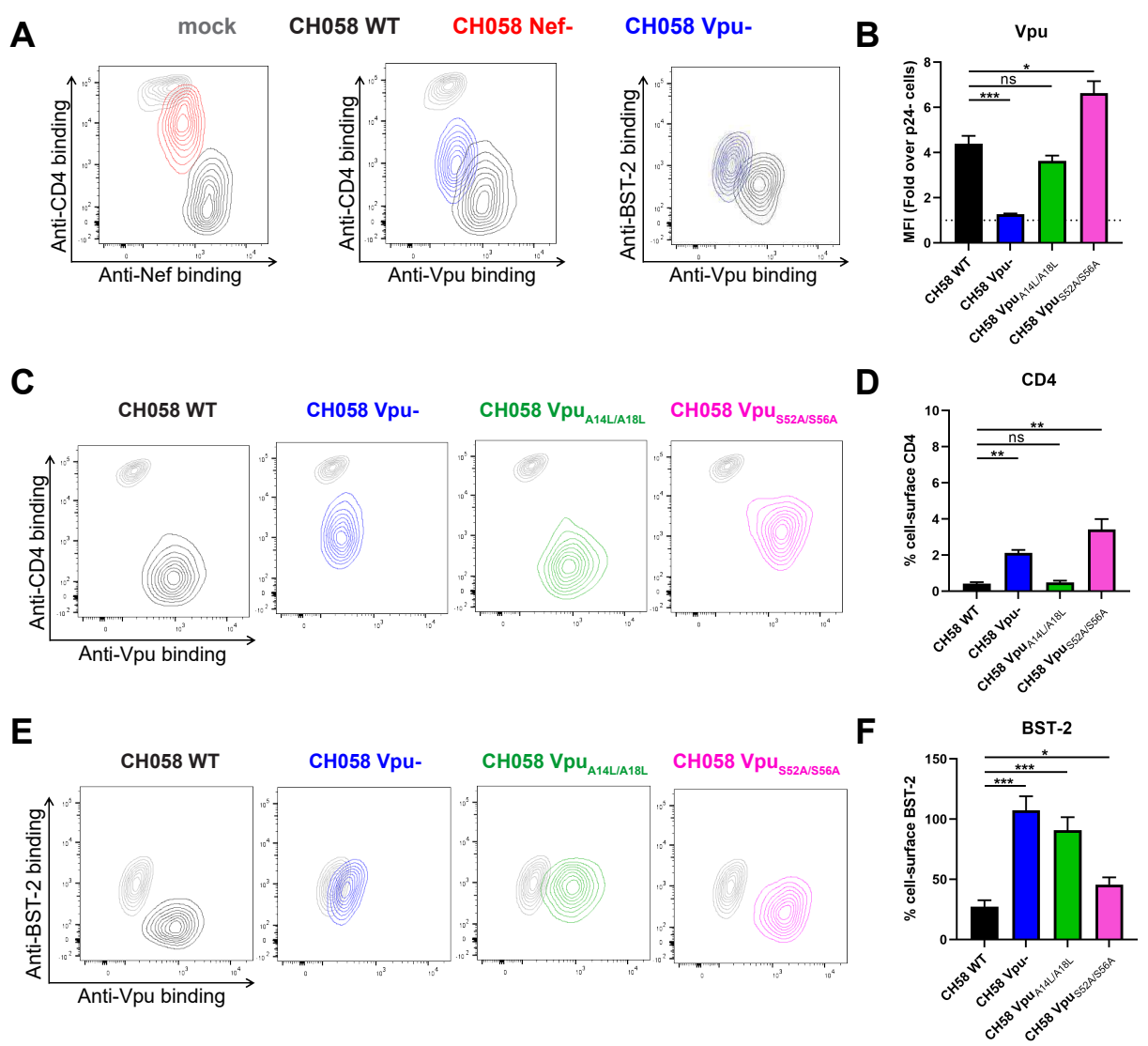

Figure 2. Concomitant detection of intracellular Nef and Vpu and cell-surface CD4 and BST-2.

Primary CD4+T cells infected with CH058 T/F WT, Nef-, Vpu-, Vpu A14L/A18L or Vpu S52A/S56A viruses were stained for cell-surface CD4 and BST-2 prior to detection of intracellular Nef or Vpu expression. (**A,C,E**) Contour plots depicting representative cell-surface CD4 or BST2 detection in combination with Nef or Vpu intracellular detection. Mock-infected cells were used as a control and are shown in grey. (**B,D,F**) The graphs show MFIs obtained from five independent experiments. Error bars indicate means ± standard errors of the means (SEM). Statistical significance was tested using an unpaired t test or a Mann-Whitney U test based on statistical normality (*, $P < 0.05$; **, $P < 0.01$; ***, $P < 0.001$; ns, nonsignificant).

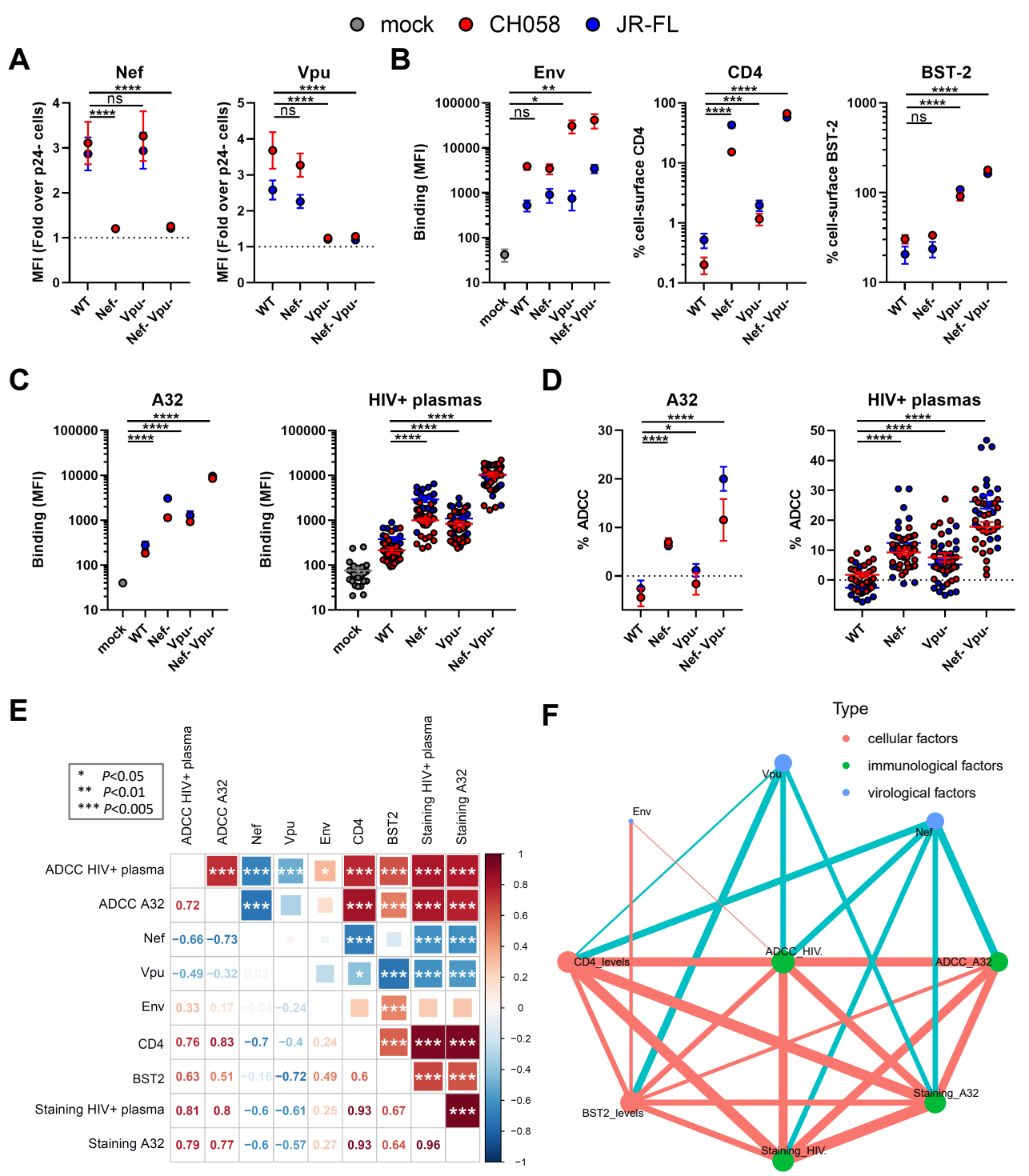

Figure 3. Nef and Vpu intracellular detection inversely correlates with the recognition of infected cells and their susceptibility to ADCC responses mediated by HIV+ plasma. Primary CD4+T cells were mock-infected (grey), infected with CH058 T/F (red) or JR-FL (Blue) viruses (WT, Nef-, Vpu-, Nef- Vpu-) and stained for (**A**) intracellular Nef or Vpu expression in combination with (**B**) cell-surface staining of Env (using the anti-Env 2G12 mAb), CD4 and BST-2. The ability of the anti-Env A32 mAb and 25 different HIV+ plasma to (**C**) recognize infected cells and (**D**) eliminate infected cells by ADCC was also measured. (**A-D**) The graphs show the MFI obtained on the infected (p24+) cell population using cells from five different donors. Error bars indicate means ± standard errors of the means (SEM). Statistical significance was tested using an unpaired t test or a Mann-Whitney U test based on statistical normality (*, P<0.05; **, P<0.01; ***, P<0.001; ns, nonsignificant). (**E**) Correlograms summarize pairwise correlations among all immunological, virological and cellular variables obtained from infected primary CD4+ T cells (shown in **A-D**). Squares are color-coded according to the magnitude of the correlation coefficient (r) and the square dimensions are inversely proportional with the P-values. Red squares represent a positive correlation between two variables and blue squares represent negative correlations. Asterisks indicate all statistically significant correlations (*P < 0.05, **P < 0.01, ***P < 0.005). Correlation analysis was done using nonparametric Spearman rank tests. (**F**) Correlation networks were generated using data shown in (**E**). Each node (circle) represents a cellular (red), an immunological (green) or a virological (blue) feature measured on infected cells. Nodes are connected with edges (lines) if they are significantly correlated (P < 0.05); nodes without edges were removed. Edges are weighted according to P-values (inversely). Red edges represent a positive correlation between two variables and blue edges represent negative correlations. Nodes are sized according to the r-values of connecting edges.

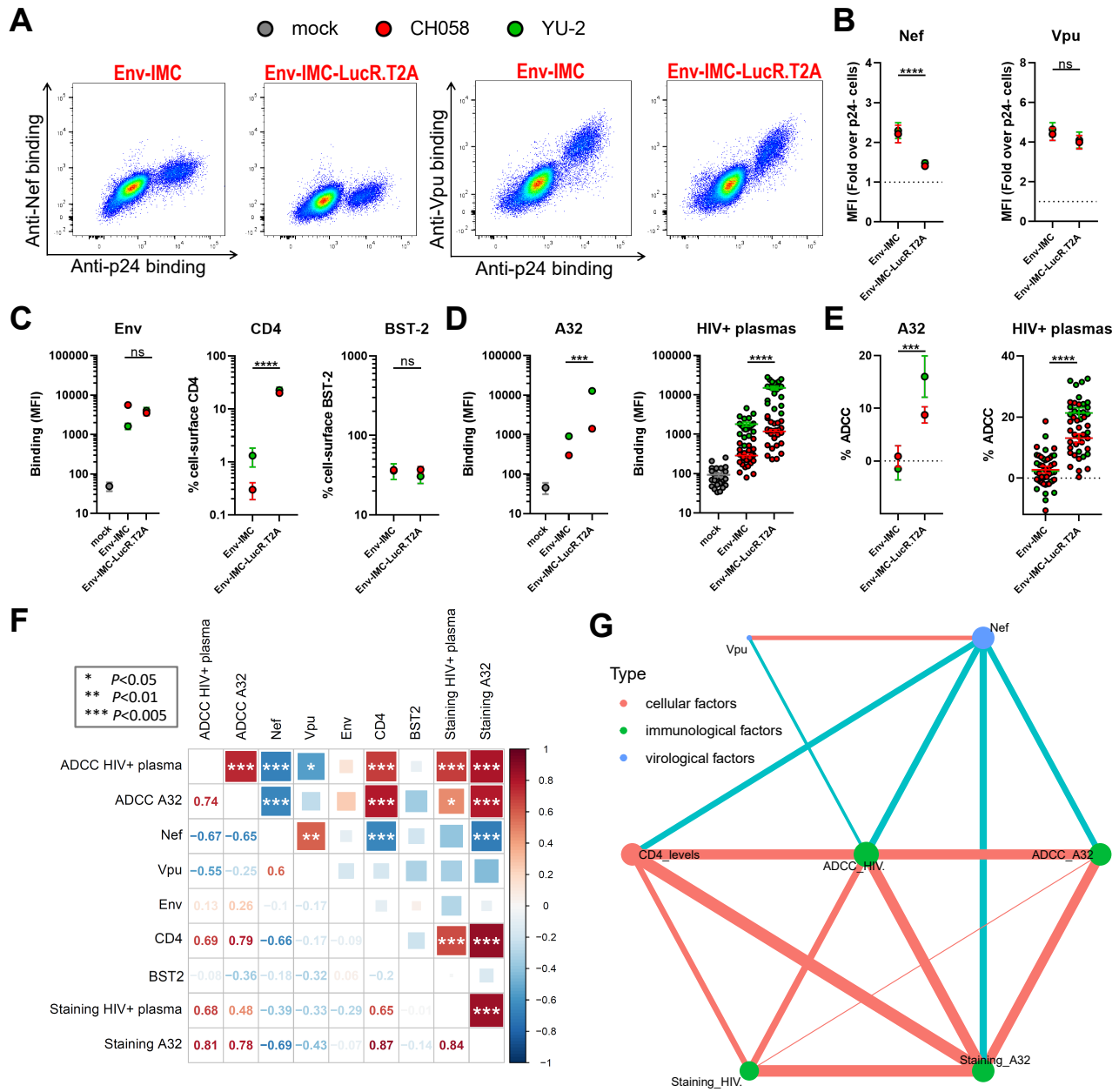

Figure 4. Lack of Nef expression in primary CD4+ T cells infected with LucR.T2A IMCs results in enhanced ADCC.

Primary CD4+T cells mock-infected (grey) or infected with chimeric IMCs expressing CH058 Env (red) or YU-2 Env (green) and expressing or not the LucR reporter gene. (**A**) Dot plots depicting representative stainings of intracellular Nef or Vpu expression. (**B-C**) Detection by flow cytometry of (**B**) intracellular Nef or Vpu expression in combination with (**C**) cell-surface staining of Env (using anti-Env mAbs 2G12 (CH058) or PGT135 (YU-2)), CD4 and BST-2. The ability of the A32 mAb and 25 HIV+ plasma to (**D**) recognize infected cells and (**E**) eliminate infected cells by ADCC was also measured. (**B-E**) The graphs show the MFI obtained on the infected (p24+) cell population using cells from five different donors. Error bars indicate means ± standard errors of the means (SEM). Statistical significance was tested using an unpaired t test or a Mann-Whitney U test based on statistical normality (*, P < 0.05; **, P < 0.01; ***, P < 0.001; ns, nonsignificant). (**F**) Correlograms summarize pairwise correlations among all immunological, virological and cellular variables obtained from infected primary CD4+ T cells (shown in **B-E**). Squares are color-coded according to the magnitude of the correlation coefficient (r) and the square dimensions are inversely proportional with the P-values. Red squares represent a positive correlation between two variables and blue squares represent negative correlations. Asterisks indicate all statistically significant correlations (*P < 0.05, **P < 0.01, ***P < 0.005). Correlation analysis was done using nonparametric Spearman rank tests. (**G**) Correlation networks were generated using data shown in (**F**). Each node (circle) represents a cellular (red), an immunological (green) or a virological (blue) feature measured on infected cells. Nodes are connected with edges (lines) if they are significantly correlated (P < 0.05); nodes without edges were removed. Edges are weighted according to P-values (inversely). Red edges represent a positive correlation between two variables and blue edges represent negative correlations. Nodes are sized according to the r-values of connecting edges.

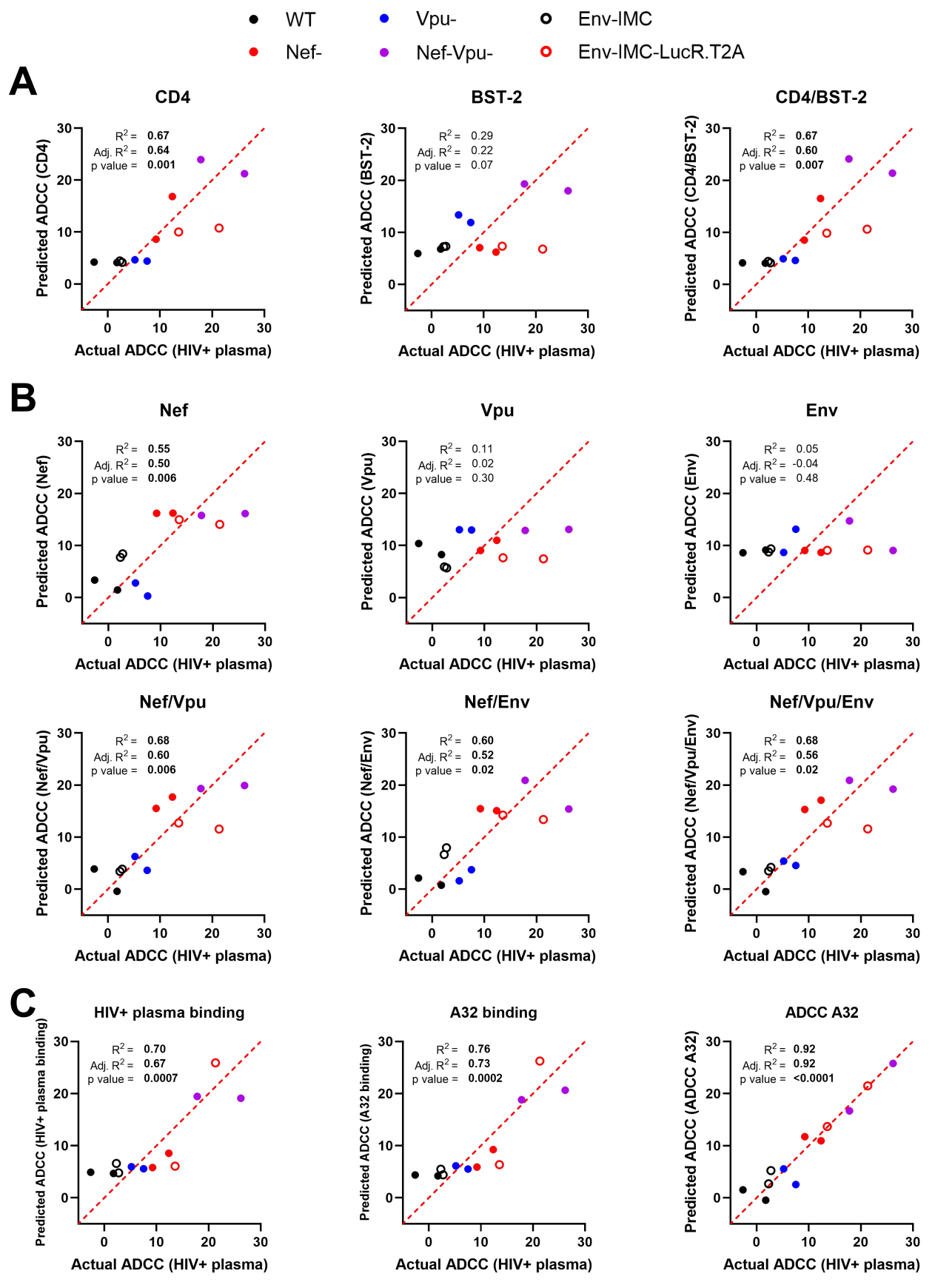

Figure 5. Prediction of ADCC responses mediated by HIV+ plasma using multiple linear regression models.

(**A-C**) Multiple linear regression analysis to identify variables that can predict the ADCC responses mediated by HIV+ plasma against primary CD4+ T cells infected by different viral constructs (WT, Nef-, Vpu-, Nef-Vpu-, Env-IMC, Env-IMC-LucR.T2A) from different HIV-1 strains (CH058, JR-FL, YU-2). Each dot represents a single virus where the average of ADCC obtained with 25 different HIV+ plasma (dependent variable) is plotted on the X axis and the predicted ADCC value based on one or more independent parameters is plotted on the Y axis. Predictors include (**A**) cellular variables, (**B**) virological variables and (**C**) immunological variables. Multiple linear regression analyses were performed using the GraphPad Prism software (version 9.1.0). P values below 0.05 are considered significant and are highlighted in bold. The coefficient of multiple correlation (R^2) indicates the goodness of fit of the multiple regression linear model. The adjusted R^2 (Adj. R^2) is used to compare the fits of models across experiments with different numbers of data points and independent variables.

Figure S1. Sequence alignment of Vpu C-terminal region from HIV-1 major clades. (**A-H**) Logo depictions of the frequency of each amino acid from the Vpu C-terminal region (residues 70-82) in isolates from (**A**) clade B, (**B**) clade C, (**C**) clade A1, (**D**) clade D, (**E**) clade F1, (**F**) clade G, (**G**) CRF01_AE and (**H**) CRF02_AG. The height of the letter indicates its frequency within the clade. The residues corresponding to the immunogen used to generate the rabbit Vpu antiserum are highlighted in blue. The 2019 Los Alamos database-curated filtered web Vpu alignment was used as the basis for this figure, which contains 5,292 amino acid HIV-1 group M sequences (including 1,819 sequences of subtype B, 1,075 of subtype C, 247 of subtype A1, 87 of subtype D, 47 of subtype F1, 80 of subtype G, 397 of CRF01_AE and 139 of CRF02_AG). Residue numbering is based on the HXBc2 reference strain of HIV-1.